JET–R(99)12

J Jacquinot et al

Study of JET Enhancements Leading to Extended Physics Operations and Fusion Performance

JET–R(99)12

Study of JET Enhancements Leading to Extended Physics Operations and Fusion Performance

J Jacquinot, C Gormezano, E Joffrin, P Thomas, H Altmann, D Borba, C Challis, A Kaye, P Lomas, C Lowry, G Matthews, F Milani, V Parail, V Riccardo, G Saibene, R Sartori, G Sips, E Solano, M Watkins.

JET Joint Undertaking, Abingdon, Oxfordshire, OX14 3EA,

December 1999

EXECUTIVE SUMMARY

At the end of 1999, which is the statutory end of the JET Project under the JET Joint Undertaking, JET will have fulfilled all its missions. Considerable progress has been achieved in the knowledge of plasma behaviour in conditions approaching those required in a thermonuclear reactor. On the basis of this recent knowledge, we have studied the enhancements required to extend the JET operating domain and performance.

The main JET programme line over the last 7 years has been the development of a valid divertor concept for ITER. Installation and exploitation, in a systematic manner, of several divertor structures has been required: successively Mark-I, Mark-IIA and Mark-IIGB. The divertors, particularly Mark-IIA and Mark-IIGB, significantly reduced the plasma volume. In spite of this, the 1997 D/T campaign has produced impressive results: Record fusion yield (16 MW peak) and record fusion energy (22 MJ in steady-state discharges) have been obtained. Alpha-particle heating has been clearly observed with alpha power in the range of a few megawatts. These results represent a significant advance in the physics of fusion plasmas. However, these studies indicate that the full potential of JET has not been fully exploited. The JET performance and operating domain can be much improved by increasing: a) **the plasma volume** (restoring the volume available before installation of the divertors), b) **the plasma triangularity** and c) **the additional power** (up to a total of 40 MW to access the threshold of high performance regimes and 50 MW to access the pressure limits). These enhancements will also benefit from the new toroidal field capability of 4 Tesla.

A 30% increase in plasma volume and higher plasma triangularity from 0.20 to 0.45 (6MA/4T) can be obtained by installing a new divertor configuration optimised for both performance and configuration flexibility and restoring the power handling capability of Mark-IIA. It will be possible to operate highly-shaped 6 MA (the present limit is 4.5 MA) divertor plasmas at 4 T. The mechanical stresses in these conditions are all within the allowable limits. The divertor design could include the possibility of testing different choices of first wall material. The new configuration is compatible with the present coil and power supply systems but require a substantial change of the in-vessel arrangements. The transformation would require about a 3-year preparation period followed by a shutdown somewhat longer than a year. Detailed scheduling studies show that the number of man entries to the vessel can be kept to an acceptable level using the JET remote handling equipment.

Increased additional power could be achieved by a combination of several methods to be chosen after a detailed study. The most cost-effective and low-risk way would be to upgrade the present Neutral Beam systems and to provide additional ICRH antennae. However, procurement of a large (≥10 MW) ECRH system could be advantageous providing additional functionality in relation to stabilising high-pressure modes and providing pure electron heating.

Performance extrapolations have been made for the ITER reference regime (steady state ELMy H-mode) and the ELM-free H-mode (transient) on the basis of actual scaling results

obtained during the last JET D-T phase (DTE1). The volume increase improves confinement and the fusion power amplification factor Q, while the additional heating power provides access to the favourable regimes. The 2 enhancements are highly synergistic (see table). In total, the fusion yield of 6 MA, 4 T plasmas are expected to be a factor 4 higher than in DTE1. The total fusion energy released in a single pulse would approach 100 MJ and **breakeven conditions would be exceeded.** The following burning plasma issues could be explored in support of the next step device:

- Stability and plasma interactions of energetic particles in conditions of substantial heating by alpha particles. In particular the electron heating source will be clearly dominated by alpha particle heating in a large core region.
- Significant in-roads towards the reactor domain in terms of normalised size (ρ^*) and plasma pressure (β_N),
- Substantially reduced uncertainties in scaling to the next step devices and validation of advanced scenarios.

	P_{fus} [MW]	Q_{tot}	β_N	ρ_i^*/ρ^*_{ITER}	Triangularity at maximum volume	Access to density
JET present size (85 m^3; 26MW)	$4.4^{(1)}$ $16^{(2)}$	0.18 0.63	1.3 1.7	2.5 3.0	0 - 0.35	$0.7\ 10^{20}$
JET present size (85 m3; 40MW)	$8^{(1)}$ $32^{(2)}$	0.2 0.8	1.7 2.4	3.0 3.5	0 - 0.35	$0.7\ 10^{20}$
JET Enhanced (107 m3; 40MW)	$22^{(1)}$ $72^{(2)}$	0.55 1.9	1.7 2.5	2 2.5	0.2 - 0.45	$1.1\ 10^{20}$

Synergetic effects of the large volume and additional power on the JET-enhanced performance (6 MA/4 T) [(1)] steady state, [(2)] transient

A programme extending over Framework Programme 6 would allow the objectives stated above to be reached. The total cost of the enhancements would represent about 5 % of the existing investments. The cost of additional heating being modular, the associated cost could be spread over the first 4 years starting in year 2000.

In summary, moderate investments in JET would allow:

a) an improvement in the understanding of plasma behaviour closer to the operating boundaries required in a reactor;

b) significant progress in fusion power production to demonstrate the availability of the necessary technology;

c) studies of plasmas with appreciable α-particle heating to be undertaken.

JET, with its size and demonstrated tritium capability, is the only fusion experiment in the world capable of reaching these goals in the decade to come.

1. INTRODUCTION

Since its creation, the JET project (under the Joint JET Undertaking) has brought considerable progress to fusion science and plasma physics. Plasma discharges have been produced in conditions close to those required in thermonuclear reactors and various divertor concepts have been successfully tested. These achievements have motivated and nourished the concepts and design of the International Thermonuclear Experimental Reactor (ITER) [1]. The JET contribution for this detailed design study has been overwhelming both to validate the physics database and as a facility to test and qualify new concepts.

Given the impressive results already performed by the JET facility [2, 3] (16MW peak fusion yield, 22MJ of fusion energy), we argue in this report that even more significant plasma physics issues could be addressed by exploiting the full potentials of the JET facility. The JET performance can be much improved by increasing the plasma volume, up-grading the additional power up to 40MW, and operating at higher triangularity. Increasing the plasma volume would allow the plasma current and the fusion gain to be increased. Increasing the power capability would allow access to high confinement modes and to assess pressure limits at full field. Finally, increasing the plasma shaping would allow operation at higher densities.

With these new configuration and heating upgrades, the fusion yield was enhanced significantly with respect to the previous DT experiments thanks to the higher plasma current. The target total energy released in a single pulse could reach 100MJ and Q could approach 2. In addition, by extending the operational domain both in β_N and ρ^*, burning plasma issues like alpha particle heating [4], pressure limits, plasma stability in presence of energetic particles can be explored in support of the next step device. Furthermore, the JET-enhanced could again substantially contribute to the extension of the physics database by reducing the uncertainties in scaling to the next step device [1] and validating the advanced scenarios [5,6].

In this report, the capability of JET operating with an enlarged configuration and heating capability has been studied. The authors have estimated the in-vessel modifications required to recover 30% of the volume of JET plasmas and have tried to minimise the tasks to be done to JET in order to keep the required procurement time of components and the shut-down time to reasonable duration.

The report is organised as follows:

- **Possible Heating Upgrades in JET** where the required additional power and possible additional heating enhancements are discussed.
- **Enhanced Plasma Configuration** discussing the enlarged volume and increased triangularity which can be achieved while keeping the present divertor coils.
- **Modelling of Predicted Performances** including fusion performance with the ELMy H-mode (ITER mode), the ELM free H-mode [5] and the advanced scenarios [6] (Optimised Shear mode).

- **Burning Plasma Physics Issues** to be investigated in Enhanced JET including: heating by alpha particles [4] and energetic particles stability effects, transport issues and macroscopic stability.
- **Divertor Requirements** where an outline of a possible divertor with high heating capability and large flexibility is presented.
- **Technical Aspects** including stress calculations for operating at maximum field and current and remote handling aspects.

2. POSSIBLE HEATING UPGRADES IN JET

The present Heating and Current drive capability in JET is as follows:

- **Neutral Beam Injection (NBI):**
  - 12MW at 80keV for more than 5 sec
  - 8MW at 140keV for more than 5 sec
  - routine capability: 16 to 18MW (in deuterium).
- **Ion Cyclotron Resonance Heating** (ICRH) from 25 to 60MHz. The launching capability depends upon plasma conditions:
  - up to 22MW in limiter plasmas
  - up to 17MW in diverted plasmas with ICRH alone
  - up to 15MW in combined heating with type III ELMs (10MW routine in Optimised Shear scenarios)
  - up to 8MW in combined heating with type I ELMs
  - ICRH can be separated for 20 sec pulses.
- **Lower Hybrid Current Drive** (LHCD) which is the only off-axis JET current drive capability:
  - up to 7MW with limiter plasmas
  - up to 3MW with ELMy plasmas but only 1MW with optimised shear plasmas with an H-mode edge.

The routine combined heating power depends upon a variety of conditions. It can reach up to 25 to 28MW in ELMy plasmas.

2.1 Required Additional Heating Power

Compared to other machines such as ASDEX-U, DIII-D and JT-60U JET is underpowered as illustrated in Table 2.1. JT60-U in Japan has more than 45MW of installed power for a smaller volume. Both ASDEX-U and DIII-D have installed almost the same amount of additional power for only one sixth and one quarter of the JET volume respectively. This lack of additional power is seriously limiting the operational domain of JET and prevents the exploitation of its high magnetic field capability.

	$P_{NBI} + P_{IRCH}$ (MW) (maximum installed power for divertor plasmas)	Installed Power Density [MW/m^3]	Upgrades in Construction [MW]
ASDEX-U V = 13m^3	20 + 6	2	2 (ERCH)
DIII-D V = 24m^3	20 + 6	1.1	6 (ECRH)
JT60-U V = 73m^3	40 + 6	1	4 (ECRH) 10 (N-NBI)
JET V = 85m^3	20 + 10	0.36	1 to 5 MW (NBI + ICRH)

Table 2.1: Power installed or under construction in major devices.

The present power capability (16 to 18MW of Neutral Beam Injection (NBI) power and up to 8MW of Ion Cyclotron Resonance Heating (ICRH) power in ELMy plasmas), has severe limitations for a fusion physics programme, as discussed in the following sections.

β_N Limits

The most significant limit is linked to the assessment of the plasma pressure limits, in particular β_N, at full field. In a pressure limited plasma the fusion power is proportional to β_N^2. However, β_N is limited by a variety of ideal and resistive MHD instabilities, including neo-classical tearing modes (NTM) (Fig 2.1). The NTM limit is a function of collisionality and finite Larmor radius effects as expressed by ρ^* (ρ^* ion Larmor radius normalised to the plasma minor radius). Such a dependence, which is important for reactor application (as will be discussed later), is still not well established. In JET, a dependence of β_N with ρ^*, but not with collisionality, has been found for ELMy H-modes. β_N limits in optimised shear plasmas do not appear to depend upon ρ^* as shown in Fig 2.2, but additional power is required for such a study.

With the present additional power on JET, β_N values up to 1.3 and 2 have been achieved at a magnetic field of 3.4T, respectively in ELMy plasmas and in optimised shear plasma, while values considered for Next Step have to be at least 2.3. Beta limits due to NTM have only been observed for maximum magnetic field values of 2.2T with ELMy H-modes and 3T with optimised shear plasma. The power required to achieve β_N = 2.3 value considered for RTO/RC ITER is shown in Table 2.2, assuming an ELMy H-mode scaling.

Higher β_N may be accessible due to stabilisation by resistive wall modes and plasma rotation. Pressure-driven ideal external modes are predicted to be fully stabilised by resistive walls with plasma rotation, thus extending the β_N limit. This effect is more pronounced for broad pressure profiles. For quickly rotating modes, the stabilising effect of the wall increases when the wall is brought closer to the plasma. In the present JET, the ratio of resistive shell over plasma radius is about 1.4 – 1.5. In the new configuration this ratio would be reduced to 1.2 due

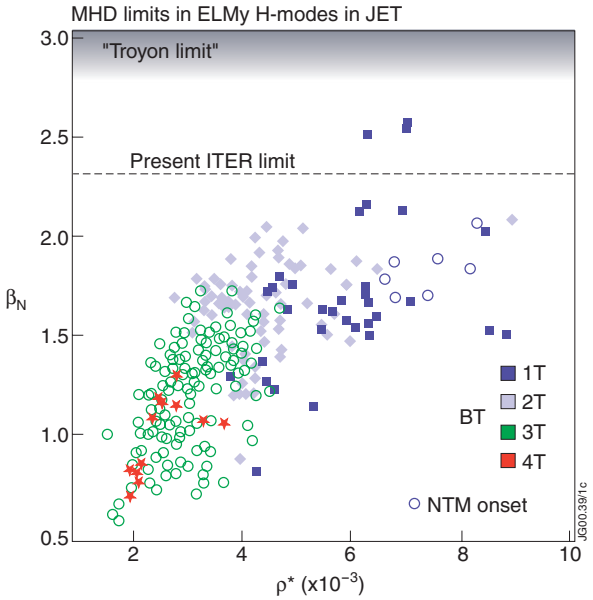

Fig 2.1: β_N versus ρ for ELMy H-mode plasmas in JET. The upper limit is the initial "Troyon" limit: β_N = 2.8.*

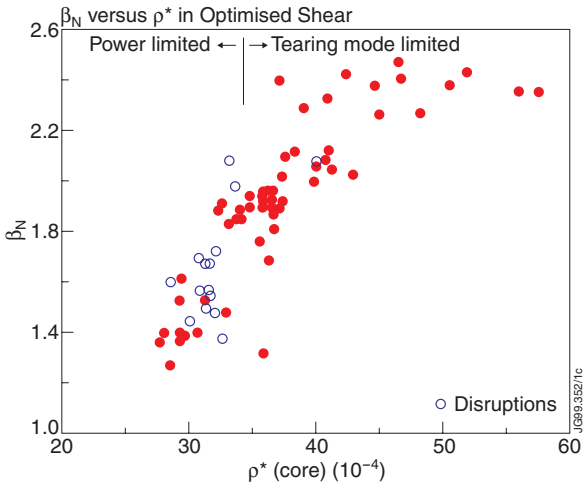

Fig 2.2: β_N versus ρ for Optimised Shear Plasmas in JET. For ρ* = ≤ 410^{-3}, lack of additional heating power prevents to assess β_N limits.*

to the removal of many out-board in-vessel components (the plasma is closer to the conductive vessel-walls). At this distance, the β_N limits could be significantly increased provided that the plasma rotation is sufficiently high. Simulations are due to be launched to quantify this effect, but already this again underlines the importance of increasing the volume and the Neutral Beam Power in the Enhanced JET.

	P_{tot} (MW) for β_N = 2.3	**P_{tot} (MW) available**
ASDEX-U (B_T = 3T; I_p = 1.5MA)	19	23
DIII-D (B_T = 2.2T; I_p = 2.0MA)	16	26
JT60-U (B_T = 4.3T; I_p = 2.6MA)	40	46
JET (present size) (B_T = 4T; I_p = 4.6MA)	70	28

Table 2.2: Power required to reach β_N = 2.3 with $n_e = 0.7n_G$, q_{95} = 3 and ELMy H-mode scaling.

Access Power to High Confinement Modes

Another important consideration is the required power in JET needed to access high confinement modes. Several types of bifurcation to improved confinement are observed in Tokamaks. The H-mode transition where an edge transport barrier occurs and the optimised shear mode (OS-mode) where an internal transport barrier (ITB) is generated in the low shear region near a

rational q surface are the best known transitions. The bifurcation, in both cases, effectively implies exceeding a power threshold. Once in H-mode, another transition to Type 1 ELMs, the ITER reference regime with even better confinement, requires about twice the H-mode threshold power. The performance projections of the next step devices are all based on the Type I ELM regime.

The access power to achieve the H-mode and the Type I ELMy H-mode is estimated from the scaling law given in the ITER physics basis (Chapter II) both for the Type 1 ELMy H-mode and for the Hot Ion H-mode. The scaling is based on the results from more than 10 divertor Tokamaks, and scales linearly with the toroidal field and the plasma area. This law also scales with the inverse of the mass as found in JET DT operation: $P_{thresh} = 0.082\ M^{-1.0} n_{20}^{0.69} B^{0.91} S^{0.96}$ (RMSE = 25.2%). Both figures for DD and DT operation are given in Table 2.3.

	Power (MW) JET (present size)		Power (MW) JET (large volume)	
	DT	DD	DT	DD
Type I ELMy H-mode ($n = 0.7n_G$)	25	30	30	36
ELM-free H-mode ($n = 0.35n_G$)	12	14	23	28
Optimised Shear ($n = 0.35n_G$, dIp/dt = 0.4MA)	27	27	35	35

Table 2.3: Power needed for accessing and sustaining the known high performance regimes at 4T either in deuterium/ tritium or in deuterium plasmas.

It must be stressed that the experiments in deuterium are essential for adjusting the operating parameters and for assessing its potential in DT operation. Therefore, the available power in JET must be compatible with DD operation. In order to give margin to access each scenario the required powers have all been increased by 50% corresponding to twice the variance calculated with the scaling law.

In the case of the OS mode, which is the most developed advanced tokamak scenario at JET, the values given in the table rely on the results of recent experiments because no definite scaling is available yet. Recent

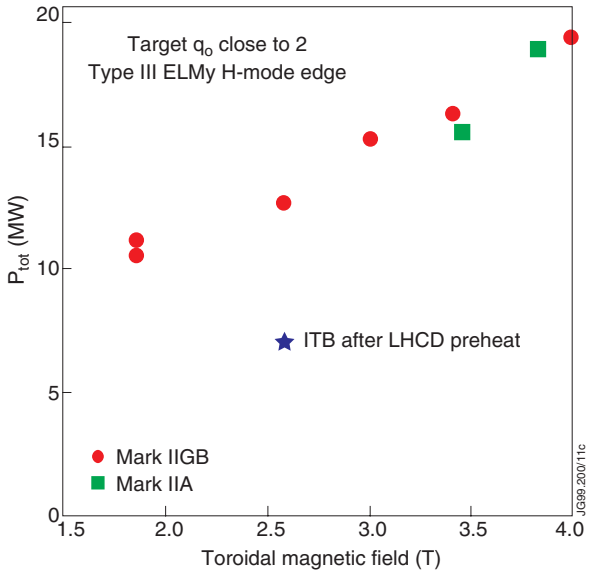

Fig 2.3: Access Power to Internal Transport Barriers in JET for similar target q profiles.

operation suggests that the power required for the Internal Transport Barrier formation also scales with the toroidal field as shown in Fig 2.3, but does not depend on mass. The access powers are calculated assuming the same dependence with the plasma area in the scaling law used for the other two modes.

The access to H-modes is not sensitive to which type of heating is used. Access to ITBs in the OS-mode has been achieved so far essentially with combined ICRH and NBI and it is very likely that central heating is essential to trigger the regime with the minimum input power. The importance of central fuelling has not been studied. Off axis current drive would be necessary to maintain the OS-mode. This could be supplied by the installed LHCD system, possibly complemented with ECRH as discussed later.

In summary, with a larger volume JET should have a total installed additional power of 40MW to access high confinement regimes and power up to 60MW to assess β_N limits at full field.

2.2 Possible Additional Heating Enhancements

Several options have been considered by the committees preparing the use of the JET facilities in the period 2000-2002. In addition to an ICRH wide band matching system which might increase the total combined power by 2 to 3MWs even in the presence of ELMs. The following enhancements have been considered:

- Enhancement of the Neutral Beam Power by 6 to 7MW. This will be done by increasing the high voltage power supply of one Octant Box from 80kV to 130kV with the same current capability.
- Enhancement of the ICRH system by installing two new 4-strap antenna modules. This would allow full use of the ICRH power plant capability even in conditions of low coupling.
- Installation of a second Lower Hybrid Current Drive (LHCD) launcher. This will also allow full use of the LHCD power plant.

The enhancement of the NBI power supply system has received the first priority. It is also in the most advanced state of preparation. It is to be noted that other enhancements such as external error field coils, a tritium extruder for the pellet centrifuge injection and diagnostics have also been considered. Other highly desirable enhancements are considered in the next paragraphs.

2.2.1 Neutral Beam Injection

A third NBI beam box could be installed re-using the third large vacuum box with its large cryopump which is presently connected to the pellet centrifuge system. The latter does not need such a large box and could easily be relocated to another position.

Such a system could be identical to the high power Octant 8 Box with its enhanced power supply capability allowing to deliver up to 15MW of power at 130kV. It could also be possible to use only 4 high current PINIs located in the central position and delivering 8MW.

Another possibility is to develop Negative Neutral Beam (N-NBI) at an injection energy of 350kV. This technique is similar to the one considered for ITER. A 500kV N-NBI system has been developed for JT-60U and is operational since 1998, although still far from its full specified performance.

Beam power depositions and current drive capability are compared for 80kV, 140kV and 350kV energies in Fig 2.4. Their respective merits are indicated in Table 2.4.

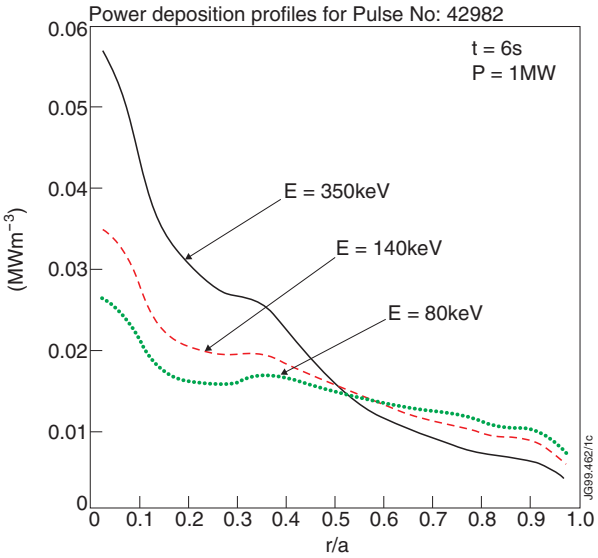

Fig 2.4: Power deposition profiles for Neutral Beams at different beam energies. Target plasma is an existing ELMy H-mode in JET.

	Positive NBI	**Negative NBI**
Advantages	• little development needed • good core heating in OS scenarios • good fuelling source	• good penetration in ELMy H-modes and ELM-free H-modes • good current drive capability in OS scenarios • similar to ITER sources
Disadvantages	• poor core penetration in ELMy H-modes and ELM-free H-modes • low central current drive capability at high density	• substantial development needed • too high central T_i in OS scenarios

Table 2.4: Comparison between positive and negative NBI. Both systems have the main advantage of mainly heating ions and will therefore substantially increase the fusion yield capability at JET.

The total current drive efficiency has been estimated for three typical plasma pulses as shown in Table 2.5.

Beam Energy	**ELM free H-mode Pulse 42976**	**ELM free H-mode Pulse 42982**	**Optimised Shear Pulse 47413**
80keV	7.8kA/MW	4.0kA/MW	24.8kA/MW
140keV	14.8kA/MW	7.9kA/MW	37.6kA/MW
350keV	46.5kA/MW	26.2kA/MW	79.1kA/MW

Table 2.5: Current Drive efficiency for three typical discharges assuming Zeff = 2.

2.2.2 Electron Cylotron Resonance Heating

An Electron Cyclotron Resonance Heating System (ECRH) presents several very interesting possibilities:

- Providing electron heating to study plasmas with electron temperatures as close as possible to ion temperatures.
- Reasonable current drive capability, especially at high electron temperature as it is typical of JET high performance plasma. This current drive capability which can eventually be combined with LHCD capability (see Section 2.2.4) could allow the issue of current profile control in the OS scenarios to be addressed.
- To address some burning plasma physics issues such as stabilisation of neo-classical tearing modes and possibly attaining regimes which allow the study of fast particle diffusion from global Alfven instabilities. This is discussed in Section 5.

Recently, the technologies of ECRH sources with the development of diamond or cryogenic windows have progressed to the industrial level for an application on JET. A system capable of coupling 10MW routinely would significantly increase the capability of studying burning plasma physics issues as discussed above. Such a system is now considered as a serious contender for reactor applications and most of the features considered for ITER can be used on JET: rotating mirrors, low loss transmission lines, etc.

The design of such a system would depend upon detailed analysis including ray tracing and current drive estimations. These studies have not yet been done. But it is estimated that ECRH waves could be launched from the low field side using a radial port at JET at a frequency ranging from 110GHz ($n_{Cut\text{-}off} = 1.5 10^{20} m^{-3}$) to 140GHz ($n_{Cut\text{-}off} = 2.4 10^{20} m^{-3}$). The exact frequency will depend upon the considered range of magnetic fields.

In order to stabilise neo-classical tearing modes, ECRH can be advantageously launched from a vertical port allowing access to rational q surfaces without too much diffraction.

This ERCH project would greatly benefit from the developments made over the last two decades by several Associations and laboratories. It could also attract collaboration from the Russian Federation and the USA. The highly modular equipment could be largely re-used on other devices if no longer required on JET.

2.2.3 Ion Cylotron Resonance Heating

ICRH is a reliable localised heating method well adapted to large Tokamaks with good fast ion confinement. Minority scenarios simulate closely burning plasmas sustained, as in a reactor, by a fast ion population in the MeV range. Its low cost technology due to high efficiency, makes it particularly ITER relevant.

If installation of two additional antennae is not considered either for economical reasons or for the installation and procurement time which would be required, all efforts have to be made

to increase antenna voltage and to make full use of the wide band matching system. A possible voltage handling limit, which is presently under study, is due to the residual second harmonic power which can build up in production voltages of a few kV above the useful voltage at the fundamental. This is due to the fact the transmission line is matched for the main frequency, but not for the second harmonic. If this is the case, proper second harmonic filters should allow voltage handling to be increased.

The present A2 antennae cannot allow a large JET volume because of their size. A possibility is to re-use the A1 antennae which does not have a proper current drive capability. To be noted that the present helicity in JET is right-handed in order to have the ∇B drift directed towards the divertor target plates. It has been shown during the MkI campaign that the H-mode power threshold is reduced in such a case, although such a difference has nearly disappeared in MkIIGB. Re-using the A1 antennae would imply operating JET with reverse helicity from the present configuration with possibly higher H-mode threshold. New antennae could be built with a design similar to the A1 antennae, in particular with an integrated picture frame, or with a new concept yet to be defined. These aspects will be discussed in Section 7.1.

2.2.4 Lower Hybrid Current Drive

The JET LHCD system has produced a large non-inductive current, up to 3MA, with the largest experimental current drive efficiency observed in tokamaks (up to 0.3 $10^{20}m^{-2}$ MA/MW). This non-inductive current drive is mainly located in the outer part of the plasma which is particularly convenient for optimised shear scenarios. LHCD only H-modes have also been produced.

The main role of LHCD is to modify the plasma current profile and not to heat the plasma. This capability has already been proven during the current ramp-up phase of the plasma, either by allowing saving transformer volt seconds (cf 7MA limiter plasmas in 1990) or by producing hollow target current profiles for optimised shear scenarios. For this, the present available coupled power of 3MW appears to be sufficient.

It is also intended to use LHCD to maintain or to further modify the plasma current profile during the high performance phase of the optimised shear discharges. But when an ITB is produced together with an ELMy H-mode edge, the scrape-off plasma density in front of the launcher decreases below the cut-off density and the reflected power increases to very high values. In effect, the plasma pedestal in these conditions is characterised by low edge density and high electron temperatures, conditions which are not suited for LHCD coupling.

Therefore, the main problem to be solved is to ionise the plasma in front of the LHCD launcher to bring the density to the required 510^{18} m^{-3} range. This is presently done by injecting some gas at about 1m from the launcher, gas which can be ionised partially by the LHCD power. But the amount of gas is not compatible with the ITB + ELMy edge. New techniques which are under study have to be developed. Following the result of such a study (gas injection as part of the launcher or external microwave ionisation source), a proposed upgrade could be considered.

3. ENHANCED PLASMA CONFIGURATION

3.1 Motivations for the Larger Volume

In the past 7 years, JET had three different divertors dedicated to specific divertor physics studies. The design of a new divertor based on the acquired knowledge would allow the operation of JET at higher power levels, with larger confinement and with higher power heat load.

With the present arrangement (MarkIIGB divertor), the plasma volume is limited to 80-85 m^3. The divertor baffles, the present ICRH antenna (referred to as the A2 antenna), the saddle coils, and poloidal limiters are seriously limiting the plasma volume on the outside. The elongation and triangularity at the separatrix are limited to 1.9 and 0.35 respectively. With this volume, the plasma current is limited to 4.5MA at 4T. For the MarkIIA, the volume was about the same, but the triangularity could be slightly higher. Also both the MarkIIA and MarkIIGB divertors are relatively closed, making it difficult to use the full volume of the JET vessel and to increase triangularity or squareness. All the in-vessel components mentioned above have been installed in the machine together with the divertor coils and the MarkI divertor. JET used to have a very large volume (about $110m^3$) before the introduction of a divertor. However, this configuration was not able to cope with high power loads, was subject to carbon blooms and had no divertor coils to control the X-point. The new plasma configuration is aiming at restoring the plasma volume to close to $110m^3$ while keeping the control capabilities of the X-point with the present divertor coils. Up to now the divertor coils have never been operated with a large plasma volume on JET.

In addition to much improved plasma shaping and wall stabilisation, higher fusion yield and confinement are the main expected benefits from the increase of plasma volume. The plasma energy content scales at β limit as $W \sim V.I_p.B_T/a$. An increase of the volume V by 25% would allow operation of JET at plasma current as high as 6MA. The energy content would be enhanced by a factor of 1.6.

Also, assuming similar β, q and ν^*, and gyro-Bohm scaling for core confinement (Wind-tunnel experiment), it can be shown that the fusion gain $Q = P_{fus}/P_{in}$ scales with increasing plasma minor radius as:

$$Q \sim B^3 \left(a^3 / R \right)^{5/4}$$

where B is the toroidal magnetic field. Therefore an increase of the minor radius by 15% leads to a gain of a factor 1.8 in thermal fusion yield.

With enhanced fusion yield, JET plasmas would approach burning plasma conditions and reactor relevant issues such as alpha heating, TAEs, and He retention could be investigated further. In addition, this increase in confinement allows bridging the confinement gap between the present JET configuration and next step configurations like those planned for RTO/RC ITER as shown in Fig.3.1. By working with plasmas at higher confinement, the statistical error bars on scaling laws can be decreased by as much as a factor of 2.

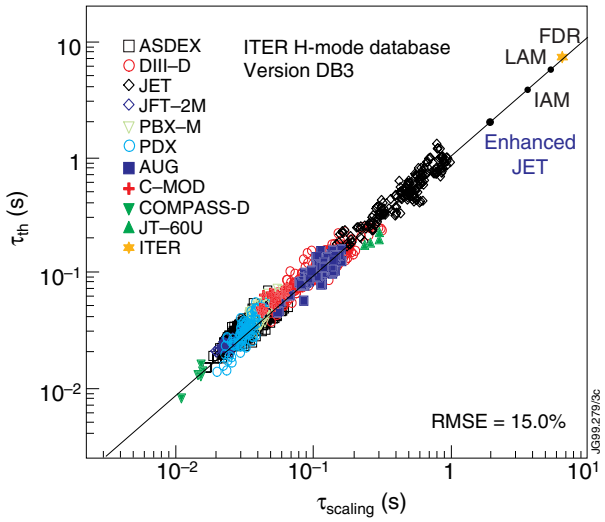

Fig 3.1: ITER H-mode database including extrapolation for the IAM and LAM versions of RC/RTO ITER as well for an Enhanced JET.

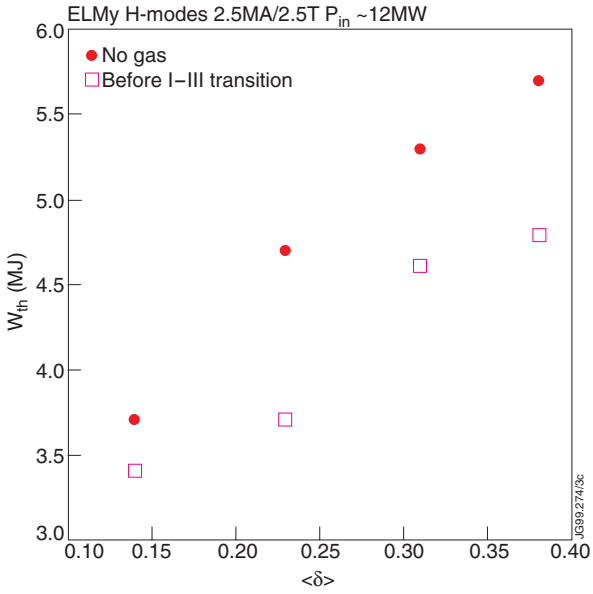

Fig 3.2: Effect of triangularity or stored energy in JET ELMy H-modes (fuelling is only from Neutral Beam Injection).

Both in JET and in other devices, the energy content increases with triangularity both for ELMy H-modes and advanced scenarios (Fig.3.2 and Fig.3.3). In particular, it is found that at higher triangularity, the operational density can be significantly increased towards the Greenwald density while keeping the same H factor. Higher triangularity also raises the edge ballooning limit and ELM-free H-modes can be significantly prolonged (Fig.3.4). Therefore, shaping capabilities of the plasma are essential for achieving maximum plasma performance.

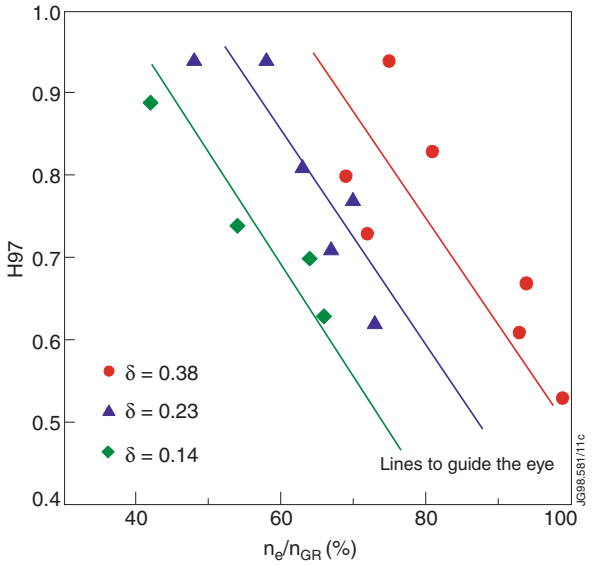

Fig 3.3: Enhanced Confinement factor (H_{97}) versus triangularity. The dependence shown on the figure has been confirmed by ASDEX.

3.2 Possible Configuration at 4T/6MA.

With the refurbishment of the in-vessel components, an optimised Ip = 6MA B_T = 4T configuration has been devised using the equilibrium code PROTEUS (Fig.3.5). In this configuration the plasma volume is maximised while keeping a minimum clearance of 2cm between the plasma and the in-vessel components. For maximum volume and elongation, the X-point is positioned very close to the target tiles (3 to 4cm above the flat divertor) and the plasma is expanded

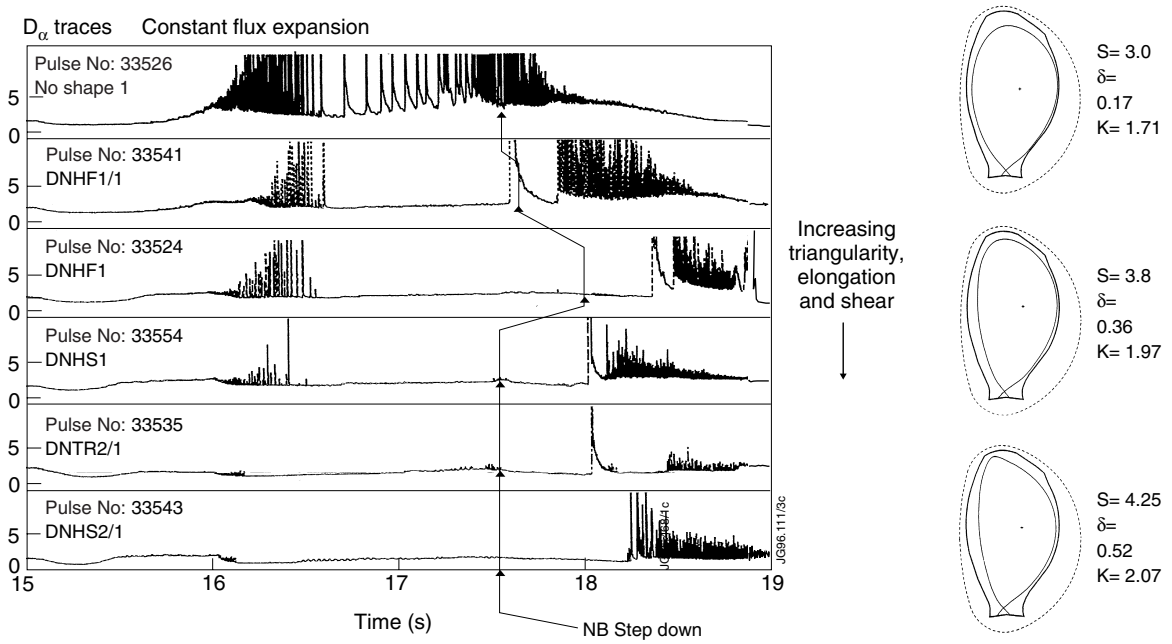

Fig 3.4: Effect of triangularity on the time duration of the ELM-free H-mode. Higher triangularity increases plasma edge stability with respect to the ballooning modes.

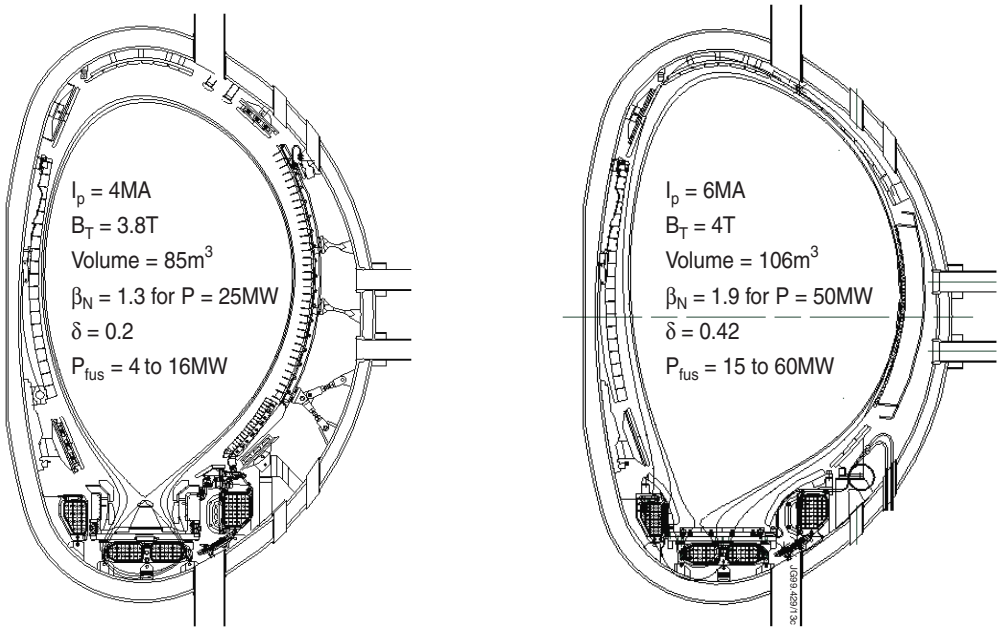

Fig 3.5: Possible plasma configuration with larger triangularity and plasma volume in an Enhanced JET as compared to the present MkII GB divertor configuration.

towards the outer wall. The volume (106m^3) is 25% higher than the maximum volume achieved with the MarkIIGB. The triangularity is maximised (δ =0 .42) by increasing the shaping currents and by locating the X-point at about R = 2.45m. Because of the X-point height (Z =-1.66m), it is now possible to significantly modify the flux expansion in the X-point region. This should help to spread the power on to the divertor plate. In addition, because of the small current present in

the lower low-field-side divertor coil, X-point sweeping remains possible as an option to control the power deposition. This configuration stays within the maximum current limits of the poloidal field coils.

The equilibrium simulation also indicates that 6.4 Webers of inductive flux is remaining at the beginning the plasma current plateau. In practical terms, the current plateau will be limited to about 5s at 6MA for the ELMy H-mode scenario because of the thermal limits on the poloidal and toroidal field coils.

The duration of the configuration also depends on the operation of JET at 4T (*see Section 7.4*). The tensile and shear stresses at the tails also limit the plateau at 4T to5s. The duration of the high power steady state phase at 6MA/4T will therefore be limited to 5s, but appears to be sufficient to achieve 100MJ of fusion power as will be discussed later.

4. MODELLING OF THE PREDICTED PERFORMANCE

4.1 Extrapolation from Existing JET Discharges

4.1.1 Method of Extrapolation.

Reference pulses have been taken from the JET database respectively for an ELMy H-mode (Fig.4.1), an ELM-free H-mode (Fig.4.2) and an optimised shear scenario (Fig.4.3). When ITER physics basis scaling laws are available, they were used for the extrapolation. Otherwise JET scaling was used, for instance for the triangularity dependence, the Z_{eff} dependence and for the advanced scenarios.

The geometrical characteristics of the equilibrium, a, R, κ, δ, are given by the Proteus equilibrium code. The elongation and the triangularity are given respectively by:

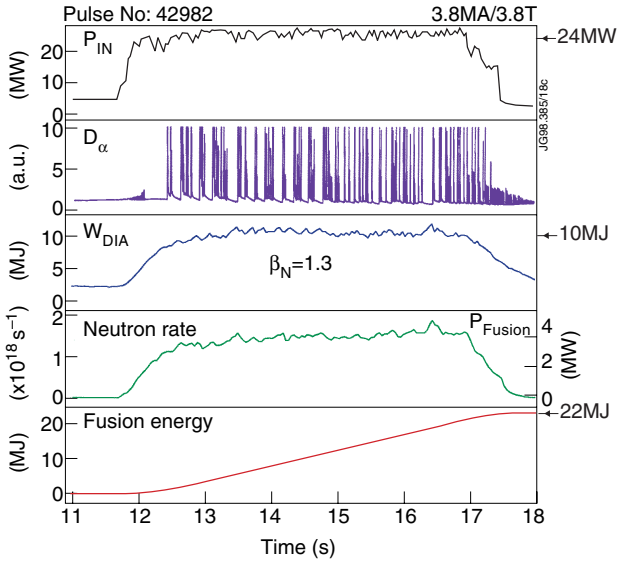

Fig 4.1: Time evolution of typical signals for the record high fusion energy yield in the JET DT phase: ***ELMy H-mode*** *(<Ti> = <Te>).*

$$\kappa = (Z_{max}-Z_{min}) / (R_{max}-R_{min}) \text{ and } \delta = (2R-R(Z_{max})-R(Z_{min})) / 2$$

where the values for R and Z are taken at the separatrix.

The line averaged density is chosen as a fraction of the Greenwald density n_G:

$$n_G = Ip / (\pi.a^2)$$

The total thermal energy content is calculated for a given input power P using the ITER98 (y,0) scaling law for ELMy H-mode as:

$$W_E = P^{0.36} . 0.0297 . M^{0.13} . (a/R)^{0.24} . B_T^{0.18} . R^{2.07} . Ip^{0.89} . K^{0.88} . n^{0.43}$$

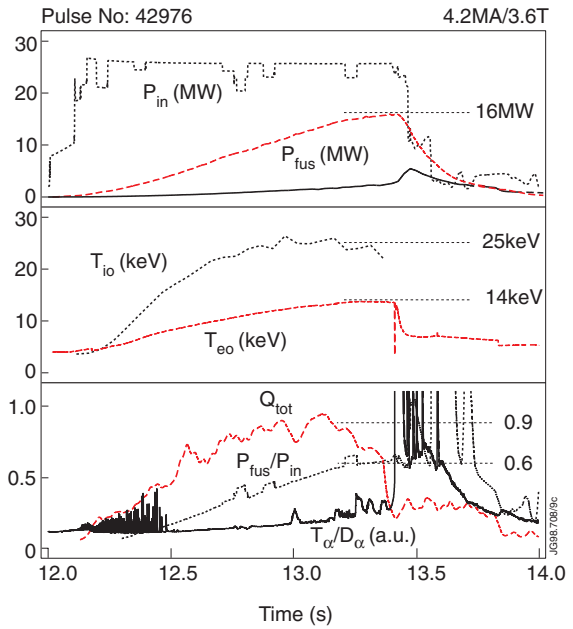

Fig 4.2: Time evolution of typical signals for the record fusion yield in the JET DT phase: ***ELM-free H-mode*** *(<Ti> = 1.6<Te>).*

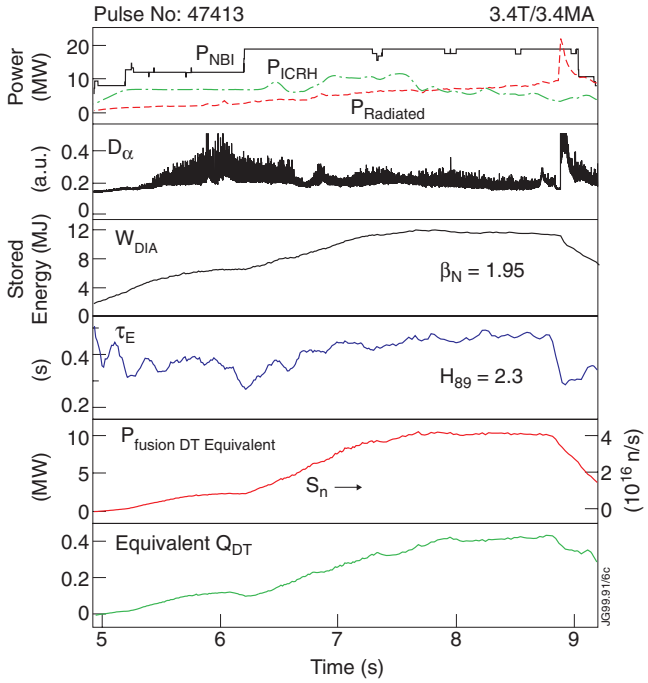

Fig 4.3: Time evolution of typical signals for the record steady fusion yield in the MkII GB JET configuration: ***Optimised Shear Scenario****.*

and for hot ion H-mode using the ELM-free H-mode scaling:

$$W_E = P^{0.36} \,.\, 0.0314 \,.\, M^{0.43} \,.\, (a/R)^{0.10} \,.\, B_T^{0.27} \,.\, R^{1.98} \,.\, Ip^{0.94} \,.\, K^{0.68} \,.\, n^{0.34}$$

From these results, the poloidal β is:

$$\beta_p = W_E / (0.15\pi \,.\, R \,.\, Ip^2)$$

Knowing β_p, the toroidal and normalised β_t and β_N, are calculated. T_i , T_e, n_i and n_e profiles are assumed to be of the form: $x = xo\,(1-(r/a)^2)^{\gamma}$. γ is taken from the reference discharge for each scenario. n_i is calculated from n_e, using constant effective plasma charge Z_{eff} and assuming carbon (Z = 6) to be the dominant impurity. The fusion power density is calculated with these profiles, using the DT cross-section and a constant peaking factor:

$$P_{fus}^{\text{th-th}} \sim n^2 \,.\langle\sigma.v\rangle(T_i)$$

This scaling is valid for the thermal-thermal power only. For the beam-thermal contribution another scaling must be used:

$$P_{fus}^{\text{beam-th}} \sim P.\,\tau_s \,.$$

where the slowing down time τ_s scales as: $T_e^{3/2} / n$. Since the D-T cross section peak is close to the injection energy (80keV), the slowing down of fast ions is assumed to be entirely on the electrons.

From Matthews scaling, Z_{eff} is expressed as:

$$Z_{eff} = 1 + 7\,P_{rad} / (S.n^2)$$

where S is the plasma area. In this scaling it is assumed that the radiated power fraction P_{rad} / P is constant.

4.1.2 Results for ELMy and ELM-free H-modes

Table 4.1 presents the performance obtained by extrapolation method described above in the enhanced JET for both ELMy and hot ion H-modes.

	Steady-State ELMy H-mode			Transient ELM-free H-mode		
	Ref pulse 42982 $V = 83m^3$ $\delta = 0.22$	$V = 106m^3$ $\delta = 0.42$, $\kappa=1.72$ a=1.08m, R=3.01m		Ref pulse 42976 $V = 85m^3$ $\delta = 0.2$	$V = 106m^3$ $\delta = 0.42$, $\kappa=1.72$ a=1.08m, R=3.01m	
B_t (T)	3.86	4	4	3.66	4	4
I_P (MA)	3.75	6	6	4	6	6
P_{in} (MW)	23.5	37	50	25.6	37	50
n/n_G	0.56	0.7	0.7	0.29	0.5	0.5
T_{io} (keV)	7.4	8.6	9.7	26	20	21.3
Z_{eff}	2.4	1.8	2.0	2.6	1.75	1.9
β_N	1.3	1.7	1.9	2.04	2.5	2.7
	1.65	15.2	15.8	9.5	63	64.7
P^{tot}_{Fus} (MW)	4.4	21	21.9	16	71.7	73.5
P_α (MW)	0.9	4.2	4.4	3.2	14.3	14.7
Q_{tot}	0.18	0.57	0.44	0.63	1.94	1.47

Table 4.1: Extrapolation from existing JET pulses

The fusion yield is increased by a factor of 4 to 5 relative to the reference pulse 42982, achieved during the D-T campaign in 1997. The high level of the predicted fusion power can be attributed to both the larger volume and the higher operating density possible with the higher triangularity of the new configuration. Also, the non-thermal fusion power is a small amount of the total fusion power, 10 and 20% respectively instead of 40 and 60%.

It can be noted that once above the power threshold (see Table 2.3), higher levels of input power do not lead any significant gain in fusion power. This is essentially due to the confinement degradation and increased dilution as the input power increases. In these extrapolations the dilution remains the most uncertain parameter. However the fusion gain for hot ion H-mode can remain as high as 1.1 even when $Z_{eff} = 3$ is assumed.

With a larger volume, JET will produce significant levels of fusion power and alpha particles thus allowing the first detailed study of burning plasmas.

4.1.3 Extrapolation for Optimised Shear Scenarios

Extrapolation of the optimised shear scenarios is more difficult in the absence of established scaling laws. In JET, comparison of an ELMy H-mode with an optimised shear plasmas at similar magnetic field (3.4T), plasma current (3.5MA) and auxiliary power (25 to 28MW) shows an increase of β_N by a factor of 1.3 and a doubling of the fusion yield (Fig.4.4). Therefore, pending further development work, the increase in fusion yield can be taken as proportional to β_N^2, thus the fusion yield increases by a factor 1.7. From extrapolations made in Table 4.1, a fusion gain of almost 1 with $P_{in} = 37MW$ and $\beta_N = 2.5$ with $P_{in} = 50MW$ could be achieved in a quasi steady-state advanced scenarios.

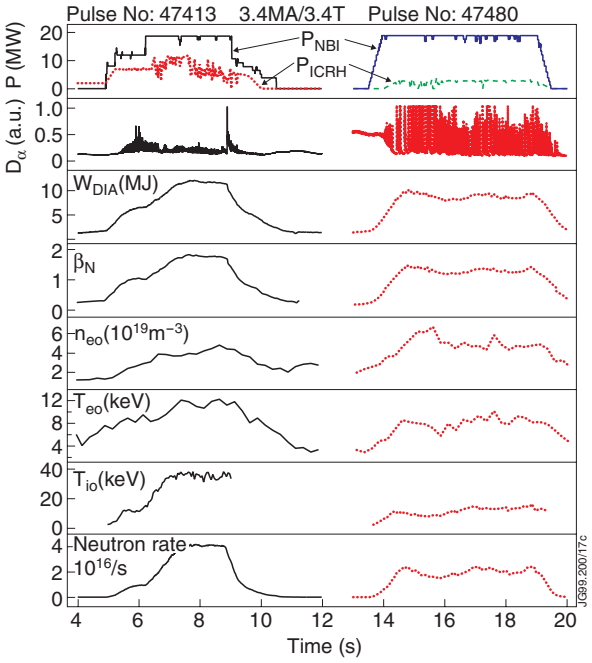

Fig 4.4: Comparison between typical signals for record D-D neutron yield plasmas with optimised shear (pulse 47413) and ELMy H-mode (pulse 47480) discharges in the MkII GB configuration (at the same plasma current and magnetic field).

4.2 Simulation with the JETTO Code

Predictive modelling of the fusion power has also been computed using the JETTO transport code with the new plasma configuration for the ELMy H-mode steady-state scenario. This 2D code uses the neo-classical transport in the edge to simulate the transport barrier and also assumes that type I ELMs are the result of reaching the edge ballooning stability condition. Elsewhere, the transport is assumed to be a combination of Bohm, Gyro-Bohm and neo-classical transport. The model satisfactorily reproduces the JET D-T pulses used to benchmark the extrapolation referred to in the previous paragraph (pulse 42982) (Fig.4.5). With the enhanced configuration, the prediction is within a few MW of the extrapolation shown in Table 4.1.

Given the agreement between the extrapolation and the prediction, JET with its enhanced plasma configuration should be able to produce about 25MW of fusion power in ELMy H-modes, or alternatively, a fusion energy in excess of 100MJ per pulse.

JETTO simulations have also been carried out for Hot Ion H-modes. For this scenario the alpha particle heating in the centre is likely to strongly dominate the electron heating from other source like the neutral beams. In the case of the reference discharge 42976, the central alpha heating was about twice as large as the neutral beam heating. The simulation indicates that the power deposition (Fig.4.6) from alpha heating will be increased by a factor of 3 with respect to the reference discharge 42976. The neutral beam heating to the electrons in the plasma core will

therefore represent a very small fraction of the total electron heating (about 15%) making possible the study of burning plasma physics relevant to reactors.

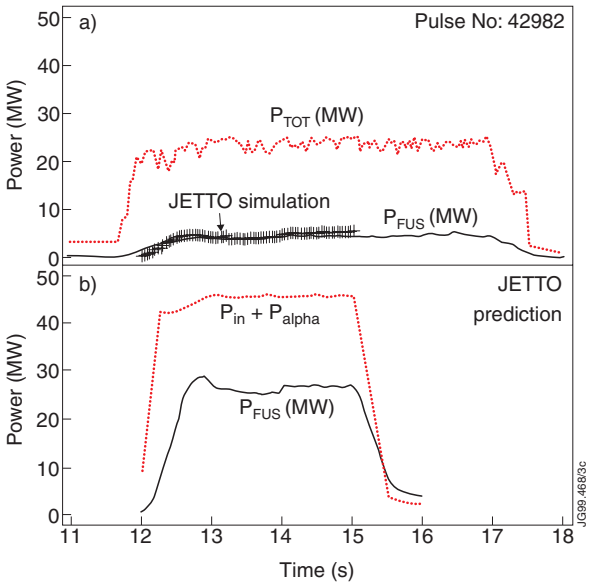

Fig 4.5: (a) JETTO simulation of record DT energy fusion yield in JET (ELMy H-mode). (b) JETTO simulation of a 6MA, 4T ELMy H-mode in an Enhanced JET configuration with P_{in} = 37MW.

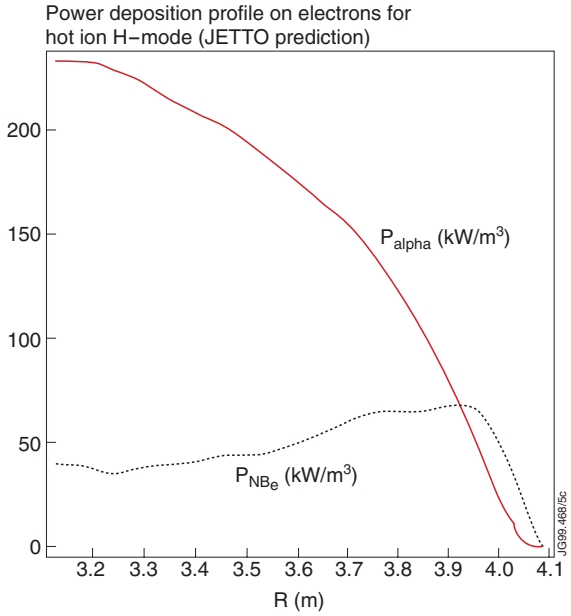

Fig 4.6: From JETTO simulation of Hot ion H-mode. Neutral Beam Power deposition on electrons compared with the alpha heating power deposition.

5. BURNING PLASMA PHYSICS ISSUES

A burning plasma experiment has, as a primary objective, the investigation of new physics associated with significant heating by 3.5MeV alpha particles born from the D-T fusion reaction. Significant progress has been made in recent years, in particular in JET DTE1 experiments, several MW of alpha particle heating were produced. In order to access reliably and assess the burning plasma regime, experiments need to be done at very low ρ^* ($\rho^* = \rho_i/a$).

Modelling of an Enhanced JET with an anticipated fusion gain of up to 2 (*as discussed in Section 4*), indicates that heating from alpha particles will not be dominant against additional heating. Nevertheless, JET, as a well diagnosed experiment, could start to address the integration of a broad range of scientific issues of interest for a burning plasma experiment. These can be divided into the following categories:

- **Energetic Particles and Alpha Heating:** Collective alpha particle-driven instabilities and associated alpha particle transport. This particular area needs diagnostic improvements (*as discussed in Section 7.5*).
- **Transport:** Transport physics in a partly self-heated plasma with dimensionless parameters relevant to a fusion reactor.
- **Macroscopic Stability:** Ideal and non-ideal MHD phenomena which limit plasma performance in a partly self-heated regime.

- **Power and Particle Handling:** Transient and steady-state heat loads, tritium retention, divertor solutions and coupling of core and edge physics at reactor scale.
- **Plasma Control:** Methods for controlling and sustaining partly self-heated plasmas on various time scales: MHD stability and feedback control, burn and central particle control, current profile control.

5.1 Heating by Alpha Particles and Energetic Particle Effects on Stability

Significant heating from alpha particles has been established in the DTE1 campaign at JET with an alpha particle heating power of up to 1.2MW with $P_\alpha/(P_{add} - P_\alpha) \sim 0.2$. In spite of these relatively low values, alpha heating was unambiguous as shown in Fig.5.1. The record fusion power pulse (Fig.4.2) had the highest plasma energy content ever recorded. In an Enhanced JET, the alpha particle power might range from a steady-state value of 4MW to a transient 14MW with $P_\alpha/(P_{add} - P_\alpha)$ ranging from 0.3 to 0.75 respectively. A much better assessment of alpha particle heating physics will be possible in such conditions.

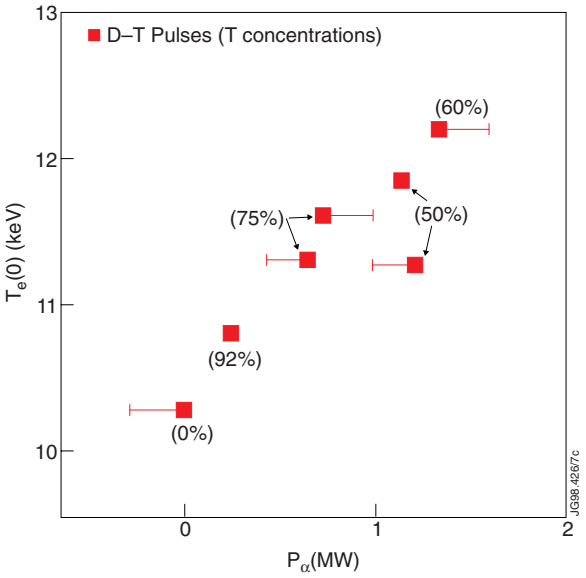

Fig 5.1: Electron temperature as a function of the alpha power in JET DT experiments.

In magnetically confined plasmas, a universal instability mechanism is active if the phase velocity of a wave is less than the diamagnetic velocity of a particular species in the plasma. As the diamagnetic velocity scales as the energy of the species, there will be a wide band of waves that can be potentially destabilised by alpha particles. Such an instability is harmful if the damping mechanism of the background plasma is small, causing a diffusion of the alpha particles. This can lead to direct loss of alpha particles, which is one of the main design issues for a reactor. It is therefore important to detect them as early as possible. The main concern is linked to global modes such as the Alfvenic instabilities, a particular example being the Toroidal Alfven Eigenmodes (TAEs). During the D-T campaign, it has been shown that these modes were not excited by the alpha particles. TAE modes driven by ICRH minority ions were detected in optimised shear scenarios but did not appear to have deleterious effects.

In order to assess the destabilising effects of alpha particles in an Enhanced JET, an initial estimate has been made using the CASTOR code as shown in Fig.5.2 showing the domain of unstable waves in terms of fast particle pressure as a function of the magnetic field. TAEs still appear to be marginally stable, because of Landau damping even for a hot ion ELM-free H-mode. However it should be noted that:

- Some theories predict that the growth rate of these modes increases with electron temperature. Therefore, heating electrons with Electron Cyclotron Resonance heating could allow the instability domain to be entered.
- The growth rate also increases with the value of the central magnetic safety factor (q_o^2) and optimised shear plasmas may constitute an ideal target for the study of such instabilities. Further modelling to identify the stability domain is progressing.

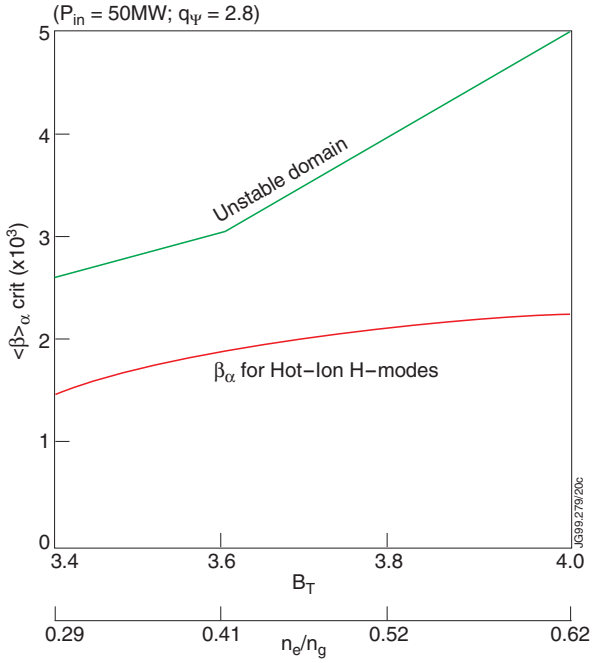

Fig 5.2: Alpha pressure as a function of density/or magnetic field from CASTOR code. β_α is calculated for an ELM-free H-mode with Pin = 50MW and a fixed q at the edge (2.8).

Energetic alpha particles also modify ideal and non-ideal MHD modes. This effect can be either stabilising or destabilising as already observed with fast ions produced with ICRH in JET and other machines. An example of this is the detrimental effect of the giant sawtooth instability after the normal sawtooth instability was stabilised by energetic particles. Other instabilities are finite larmor radius modifications of ballooning modes at high temperatures and their resonant interaction with circulating or trapped alpha particles. These resonances typically have the effect of destabilising the modes below the ideal stability limit when the diamagnetic frequency exceeds the mode frequency. But these fast ions are non-isotropic and some theories predict a significant difference between stabilising effects of isotropic and non-isotropic fast ion population. Here also, predictive studies for an Enhanced JET should be made but it is likely that a comparison of experimental effects between alphas and ICRH induced fast ions will be essential. These and other non-ideal effects relevant to fusion plasmas, effect of thermal and fast particle confinement and their role in determining the plasma pressure profiles will be important issues to address in a burning Enhanced JET plasma experiment. Their study would require the installation of specific alpha particle diagnostics (*see Section 7.5*).

Due to the larger volume and higher input power from NBI and ICRH, losses of fast ions will be significantly increased in the Enhanced JET. A large number of fast alpha particles will also be produced in D-T operation. It is therefore essential to examine the fast ions in the local mirrors of the ripple. This point shall be investigated in more detail using trajectory codes to determine the precise location that these particles strike first wall components. For this reason, the installation of claddings has been included in the conceptual design and in the in-vessel tasks to protect the vessel against fast ions.

In addition to heating and stability effects, it is also to be noted that the effect of alpha particles on the pressure profile and the subsequent modification of the current profile begins to be noticeable. A first assessment of the important issues of the effect of the alpha particles on the current profile could be done in an Enhanced JET.

5.2 Transport

The key transport issue to be addressed for any proposed burning plasma experiment is the degree of confidence which exists in extrapolating current performance levels to new regimes of dimensionless parameter (ρ^* and collisionality, υ^*) required to achieve a high fusion gain. Although uncertainty can never be completely removed, a great deal of effort has gone into strenghtening empirical scalings with first principles models of plasma confinement in order to enhance confidence in being able to extrapolate to new regimes of dimensionless parameters.

As already discussed in Section 4, the anticipated gain in confinement in an Enhanced JET will bridge the gap between existing tokamak experiments and Next Step devices. Uncertainties for extrapolation will be substantially reduced (see Fig.3.1).

In Fig.5.3, various scans in density, magnetic field, power and plasma current have been made to define the operational domain in a ρ^* and β_N. It shows that the gap between today's databases and the various options of ITER-RC can be filled.

This can be illustrated in the fusion accessibility domain shown in Fig.5.4 where β_N is plotted against $I_p.B_t.R^{0.5}$ which is a measure of the fusion gain. It shows the substantial step in fusion power and β_N capability as compared to today's experiments.

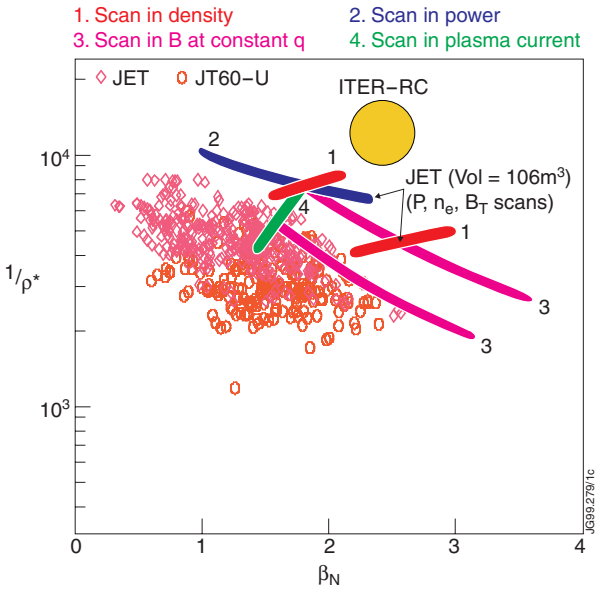

Fig 5.3: β_N versus Ip $B_T R^{0.5}$. This represents the fusion accessibility domain for ELMy H-modes and optimised shear scenarios (dotted line) in an Enhanced JET. Dashed curves represents constant fusion power.

Other important transport issues which could be addressed with an Enhanced JET are as follows:

- Effect of shaping on global confinement. To study the importance of strong shaping on the H-mode pedestal height and global confinement at small ρ^* (*as already discussed in Section 2*). Strong shaping (high triangularity) increases the pedestal height, most likely due to an increase in the threshold pressure gradient for onset of the ELMs. The new ITER-RC design incorporates stronger shaping in response to criticism of the ITER-FDR design. The JET enhanced will provide a test of the visual step.

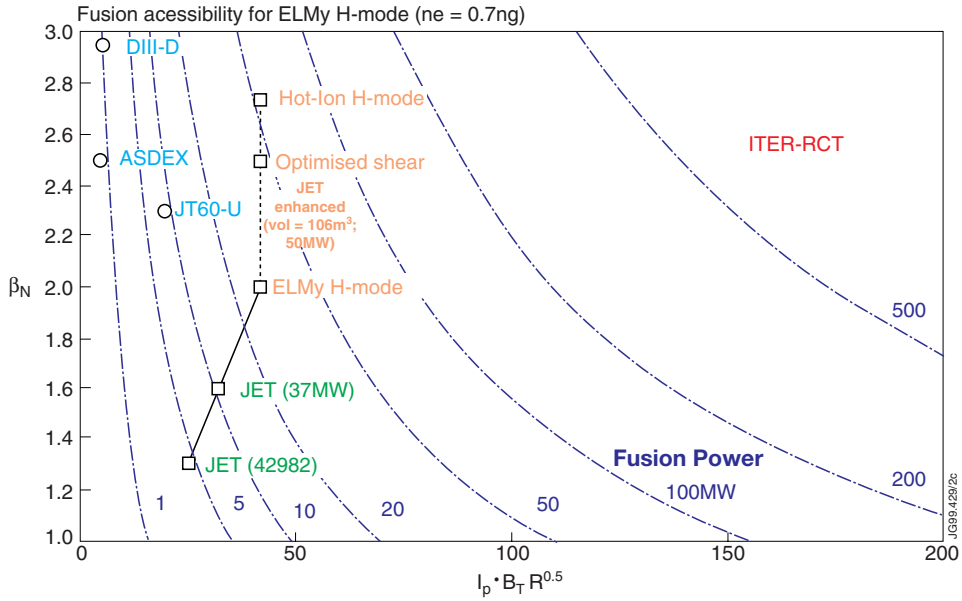

Fig 5.4: 1/ρ versus β_N for present experiments in JET and JT-60U. ρ* already achieved in these two devices are the lowest obtained so far. An enhanced JET will allow to bridge the gap between present data and ITER domain.*

- ρ* scaling of the width of the ITB in normalised co-ordinates leads to similar H-mode issues for enhanced confinement at large scale.
- Size scaling of τ_E on ρ*, E_r shear, isotopic mass and plasma density ($n \sim n_{GW}$). With the inclusion of flow shear, the scaling of confinement with size becomes a subtle issue because the net shearing rate may degrade with machine size, somewhat off-setting the favourable scaling expected with ρ*. First data are reported in Fig.2.2.
- Electron thermal transport in ITB plasmas and maintenance of ITB with significant electron heating by alpha particles. Initial results have been obtained in JET by producing ITBs with equal electron and ion temperature but with somewhat degraded performance. It will be interesting to study high performance ITBs in optimised shear plasmas with substantial electron heating.

5.3 Macroscopic Stability – Limiting High β Instabilities

The development of plasma configurations with both a high-energy confinement and high plasma beta is one of the driving objectives of the tokamak research programme. These two requirements are essential for achieving fusion energy production in a device with low enough content to be economically viable. The major limitation of most configurations are imposed by MHD stability limits which constrain plasma beta and hence fusion power density. Most of the effects have already been observed in JET, but obviously in a limited parameter range due to the lack of additional heating power preventing access to high confinement regimes at full magnetic field.

By far the dominant MHD issue is the role of neo classical tearing modes in limiting plasma performance. The NTM mode is a metastable mode for β_N that exceed a minimum value. The actual stability threshold depends upon seed island formation and width which are still being studied. The minimum beta for instability to exist is thought to scale with ρ* (at constant

υ*) which would extrapolate to lower beta in larger tokamak devices, as discussed in Section 2 (Figs.2.1. and 2.2.). The ρ* scaling is essentially empirical. There is some theoretical work to support this scaling, but the theory is highly contentious and the question remains open. Another consequence of ρ* scaling is the possibility of multiple overlapping tearing modes which can further enhance thermal transport. The evidence for a favourable υ* scaling is less compelling and there is very little theoretical support for this scaling. It is therefore important to extend the assessment of MHD limits to the lowest possible value of ρ*, i.e. at the full capability of an enhanced JET. A recent q_{95} scan was obtained by varying B_T. This is showing a fall in β_N fo $q_{95}>3$ corresponding to constant β_p which governs the drive for NTM growth. Also for $q_{95}<3$ there are sharp falls in threshold. This observation favours the operation at q_{95} slightly above 3 and therefore with the increase of volume to operate JET at 6MA/4T instead of 4.5MA/4T, as is the case with the present volume. It is also to be noted that an ECRH system could be used to study stabilisation of neo-classical tearing modes in reactor relevant regimes.

In the optimised shear regimes, edge kink/ballooning stability is particularly important to high β_N regimes with large bootstrap fraction. Optimised shear plasmas have large pressure gradients and elevated central safety factor. These states are particularly susceptible to MHD instabilities in the transport barrier and the plasma edge. This is illustrated in Fig.5.5 for JET optimised shear plasmas. With properly tuned optimised shear discharges, β_N is limited either by high n tearing modes or by the lack of additional heating power. Confinement versus β_N is shown in Fig.5.6 for JET optimised shear discharges. At lower field, β_N is limited to 2.5 by tearing modes. At higher field, lack of additional heating power prevents the attainment of the high values of the product H x β_N required for advanced scenarios being reached. The beta limit

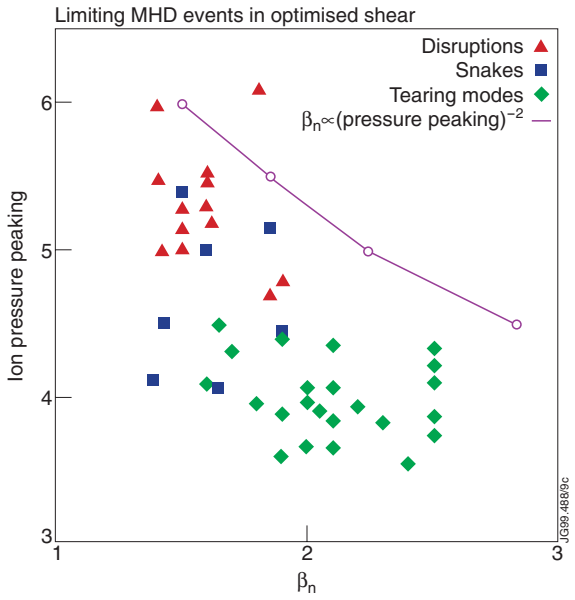

Fig 5.5: Ion pressure peaking versus β_N in JET optimised shear plasmas. Disruptions (kink modes) and snakes prevent obtention of high performance steady plasmas.

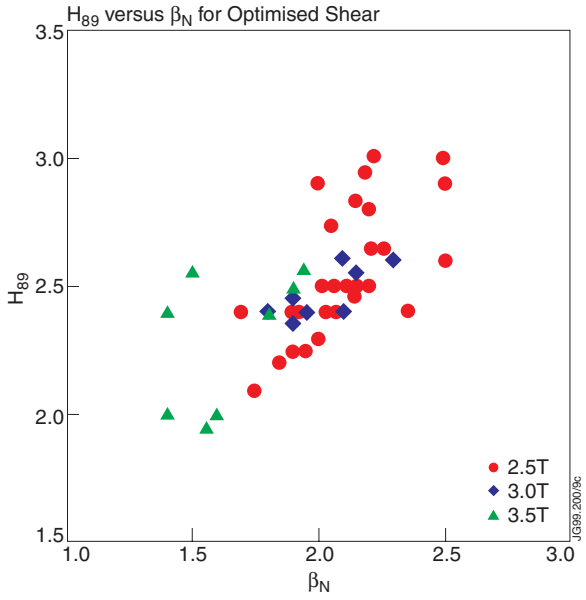

Fig 5.6: H_{89} as a function of β_N in JET optimised shear scenarios. Above 3T, betas are limited by the available additional heating power.

dependence on ρ* shown in Fig.2.2 also stresses the importance of higher power capability to assess this dependence.

Here again, a potential solution to this problem is to enhance the stability of high beta profiles with strong shaping (high triangularity). Strong shaping in an Enhanced JET will allow such effects to be assessed. Eventually such benefits should allow the domain shown in Fig.5.6 to be substantially increased.

5.4 Other Aspects

Several other aspects of burning plasma physics issues can also be studied such as scaling of advanced scenarios with Internal Transport barriers (power dependence, confinement scaling, ρ* dependence) and tritium transport issues. Helium retention and fuelling optimisation can also be studied in reactor relevant regimes. The high field side pellet launcher recently installed on JET, could be adapted if successful, to tritium operation.

Without more profound and costly modifications, the time duration of the high power pulse will be limited to 5-8s. Therefore, only the quasi steady-state aspects of high performance plasmas (MHD stable pressure and current profiles) can be studied.

6. DIVERTOR REQUIREMENTS

The past experience of JET has proven the benefit of the high degree of flexibility in divertor configurations. JET has operated successfully with three different divertors from the very open MkI to the closed MkII GB. The design of the new divertor will rely on this long experience, which shows that a narrow and deep divertor does not provide significant advantages on plasma purity but takes valuable plasma volume. The first objective of the new divertor is to allow the study of a large variety of plasma configurations. In particular, the requirements of a plasma configuration with high volume and high shaping capability demands that the X-point position be lowered and moved radially inward to increase triangularity. This can be achieved using a flat divertor with bi-directional tiles. Once the magnetic configurations are optimised, it should be possible to modify this divertor with remote handling (Fig.6.1) to adapt its heat extraction capability to high confinement regimes, D-T operation and high power loading. A flat

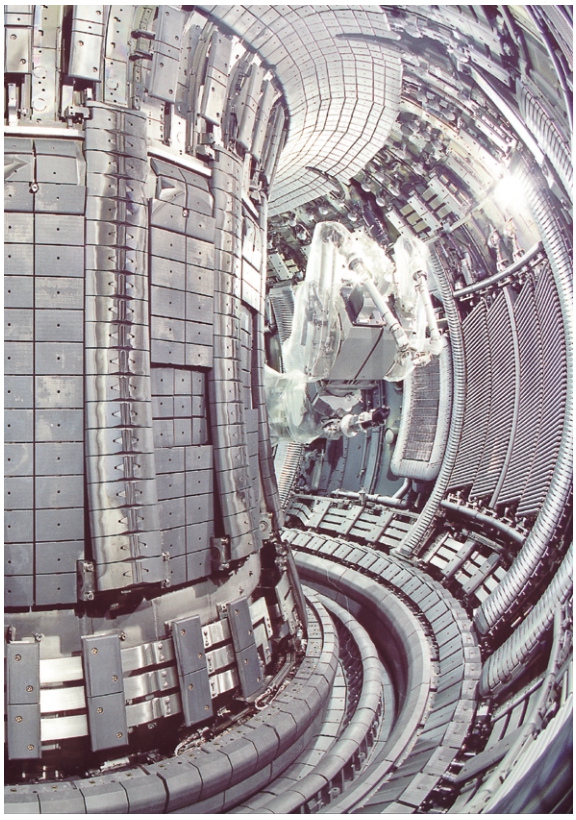

Fig 6.1: View of the remote handling boom at the end of the MkII GB installation shutdown.

divertor with bi-directional tiles satisfies the first requirement. Therefore, the main constraints arising from the operation of a 50MW heated plasma with a flat bi-directional target divertor are reviewed.

6.1 Main Divertor Components and Other In-Vessel Components

In this divertor design study (Fig.6.2). we consider the manufacture of a new base plate similar to that used for the MkII divertor. This new supporting structure comprises of 6° sectors 800mm wide. Each sector of the base plate would be pre-assembled with the tile carrier and bi-directional CFC tiles of approximately 400x200x40mm. This tile size is technically feasible at reasonable cost and is compatible with the size of the 6° sector (4 tiles per sector). The base plate is designed to be transported in modular sections into the torus by remote handling. In this conceptual design, the supports for the inner and outer tiles are hinged on each side of the base plate, the side tiles being supported at the top by an inner and an outer ring (Fig.6.3). These tiles have to be bi-directional in the toroidal direction and can be made in one piece. The inner and outer rings are mounted on the top of the clamps of divertor coils 1 and 4 to form full structural rings. To comply with the flexibility requirement, the divertor will be designed to be fully compatible with the remote handling capability present on JET. In particular, the tiles are planned to be easily removable to implement new tile geometry or material (like tungsten or molybdenum).

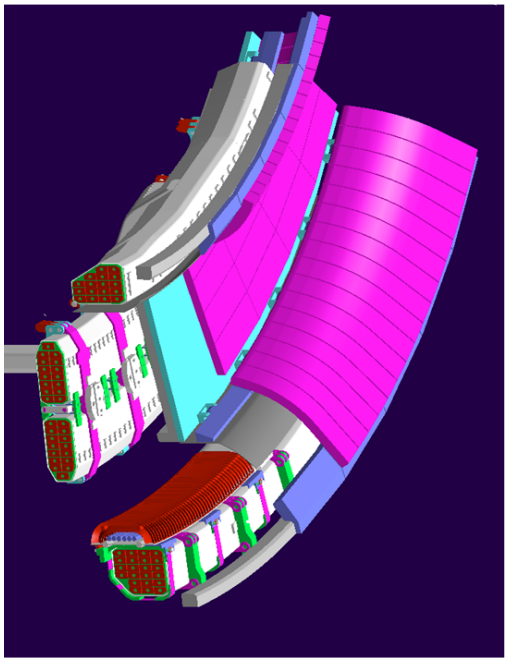

Fig 6.2: Impression of a possible new divertor plates in an Enhanced JET.

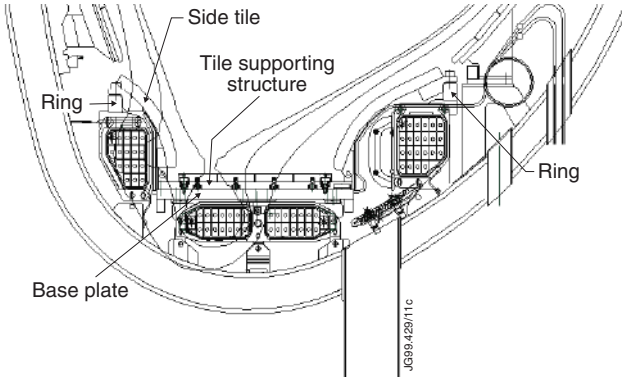

Fig 6.3: Side view of the possible tile support structure in an Enhanced JET.

In the design, both the four divertor coils and the cryo-pump are preserved. Therefore, the present X-point control and pumping capabilities will remain the same with the new divertor design.

In addition to the divertor, other in-vessel components are to be removed to make room for a larger plasma volume on the outboard side. These are the present poloidal limiters, the saddle coils, the LHCD coupler, and the ICRH A2 antennae (to be replaced by A1 antennae, *see Section 7*). A first assessment of this work is described later in Section 7.2.

6.2 Power Handling.

For H-mode plasmas the average heat load on the outer target is 2.5 to 3 times larger than on the inner target. However, if the toroidal field is reversed as it would have to be if the A1 ICRH antenna is used (see technical section) the power load is almost balanced between the outer and inner targets (1 to 1.5 ratio). Assuming a maximum input power of 50MW, and a radiated power fraction of 0.4, the power heat load on the divertor is 30MW distributed between the inner and the outer target as indicated in Table 6.1:

For 50MW of input power	**Power load on the inner target**	**Power load on the outer target**
$B_T > 0$	12-15 MW	15-18MW
$B_T < 0$	8-10 MW	20-22MW

Table 6.1: Power load on targets for different orientation of the magnetic field

Therefore the outer target is the more critical if the field is not reversed. On the other hand if B_T is positive, a power load of 15MW at high triangularity may become difficult to handle because of the off-axis position of the X-point. A large fraction of the power will then be deposited onto the inner side plates of the divertor.

Given the above power loading per leg, the local power flux on the tiles will depend on the power decay length λ_q, on the flux expansion (see Technical Section 7.3) and on the geometry of the tile. This particular point shall be examined using a set of equilibrium configurations with different X-point positions and flux expansions and specific codes to optimise the profile of the tiles. These configurations have to be compatible with the X-point sweeping as an option to spread the power on the divertor tiles. Because of the bi-directionality, the tile profiles must be symmetric in both the poloidal and toroidal direction. Moreover, experience with previous divertors on JET has demonstrated that the edge of the tiles should be shaded to avoid excessive local heat and carbon blooms on the leading edge of the tiles. Large tiles like those planned (400 x 200 x 40mm) are particularly suitable for using chamfers. Flat top roof tiles are therefore the most likely candidate to comply with the power load requirements.

Due to the anisotropic thermal and mechanical properties of the carbon fibre material, the orientation of the tile has also some very important consequences on the power handling. Along the fibres, the thermal conductivity is usually 5 to10 times higher than across. On the other hand, the thermal expansion in the fibre direction is one order of magnitude less than across the fibres.

The direction of the tile will therefore determine the minimum possible gap between tiles and the spread of the power by heat conduction. Given these characteristics of the tiles, two options can be considered:

- Tiles oriented in the poloidal direction (making 2 tiles in the poloidal direction and 120 in the toroidal direction to cover the whole divertor). In this case, the toroidal gaps will be at least 3mm and there will be only one poloidal gap. In addition, the peak heat load at the strike points can be significantly spread radially by heat conduction in the direction of the fibres.
- The tiles orientated in the toroidal direction (4 tiles in the poloidal direction and 60 in the toroidal direction). The toroidal gaps can be as small as 1mm and there will be 3 poloidal gaps of at least 3mm.

In addition to these options, the on-going detailed study shall also take into account other mechanical effects such as the bowing of tiles and their fixation to the base plate support.

6.3 Cooling Aspects

Because of the input power increase up to 50MW, cooling in between pulses needs to be considered. Assuming 15MW per leg as previously, the total energy dumped in the divertor for a 10s pulse is 300MJ. Due to the size of the tile (400x200x40mm) and to the small X-point height (a few centimetres above the target for large volume plasmas), two cases need to be distinguished: either the two strike points are on separate tiles or they strike the same tile. In the first case, each row of tile should absorb 150MJ, in the second 300MJ.

After heat diffuses in the tile (typically 17 to 70s), the average temperature of the tile corresponds to the adiabatic temperature rise required to absorbing the discharge energy. The increase of the tile temperature ΔT is given by:

$$\Delta T = E / \left(\rho \, V \, C_p \right)$$

where C_p the heat capacity, ρ the volume density and V the volume of the CFC 400x200x40mm tile. From this formula, the estimated temperature rise on one tile will be 309°C for E=150MJ and 618°C for E=300MJ. If the ambient temperature is 220°C, the tile can become as hot as 840°C when 50MW of input power is applied. This temperature is too high if the support structure of the tile is made of inconel (Inconel 713). Above 650°C, the mechanical strength of the inconel is indeed weaker. To prevent this limit, the insulation of the tile may need careful attention or the tile thickness can be increased. Also, the baking temperature can be reduced down to 150°C allowing the operation of the divertor at higher energy.

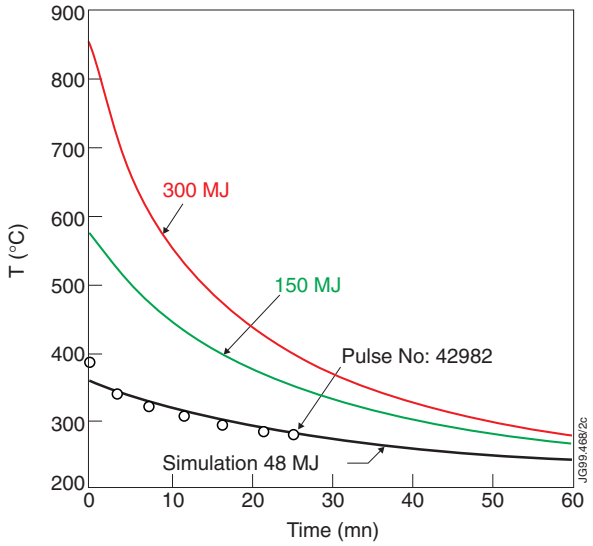

Fig 6.4: Comparison between experimental data (from thermocouples) and simulation of the cooling of the MkII GB tiles after the record fusion energy pulse (42982). The same simulation is used for the proposed Enhanced JET divertor cooling.

Assuming that tile cooling relies on radiation only, 30 minutes in between pulses are sufficient to reduce the temperature from 840°C to 370°C when the tile receives 300MJ. Therefore, there seems to be no problem in reducing the temperature to about 400°C between pulses by radiation alone (Fig.6.4). In those conditions, chemical erosion is likely to be enhanced due to the higher temperature. This should be harmless for the ELMy H-mode and probably also for the optimised shear scenario. However, the hot ion H-mode may be affected.

6.4 Pumping Aspects

As already mentioned, the present cryo-pump would be kept in the divertor; the capability for neutral particle pumping is being preserved. JET is equipped with two cryo-pumps with a pumping speed of 200 m^3/s for deuterium resulting in a pump-down time is about 1s. For helium, the pumping speed with fresh Argon frost layer is 80% of the pumping speed with deuterium.

In the last two years, JET has demonstrated the importance of reducing the by-pass leakage around the divertor. In 1996, the divertor closure was improved significantly by sealing the gaps between metal structures using aramid cloth. This had improved the ratio of leaked to pumped particles by a factor of three. This also resulted in a 50% reduction in the outer mid-plane neutral pressure. The closure of bypass gaps is therefore very important for the control of neutrals and impurities. The gap seals need to be integrated in the design to minimise as far as possible the bypass leakage around the divertor.

The pumping efficiency will also be determined by the position of the strike point relative to the corner of the divertor. The detailed design of the louvres and corners should consider the various possible equilibria to optimise their geometry with respect to neutral trajectories.

6.5 Gas Fuelling and Pellet Injector

Gas injection is presently achieved in JET by using 12 valves. Four of those gas inlets are located in the divertor. This number of gas injection modules is sufficient to control and handle the different gases required for the operation of all scenarios. Each module can inject up to 2bars per second. In addition, a specific value is also available to feed the discharge with tritium for DT operation.

JET is also equipped with a centrifuge pellet injector capable of launching pellets from both the low and high field side. The injector can deliver 4mm diameter pellets at a maximum frequency of 15Hz with a velocity ranging from 50 to 620m/s. From the low field side in typical

JET plasma (Te = 9keV, n_e = 7.10 19m^{-3}) the deposition depth is about 20 to 30cm for a 3mm pellet at 600m/s. Pellet injection experiments have recently been successfully conducted to assess the penetration from the high field side. This facility needs to be preserved and, possibly, upgraded to tritium generation to carry on the fuelling experiment on a relevant burning plasma experiment.

7. TECHNICAL ASPECTS

7.1 ICRH Antennae

7.1.1 Options

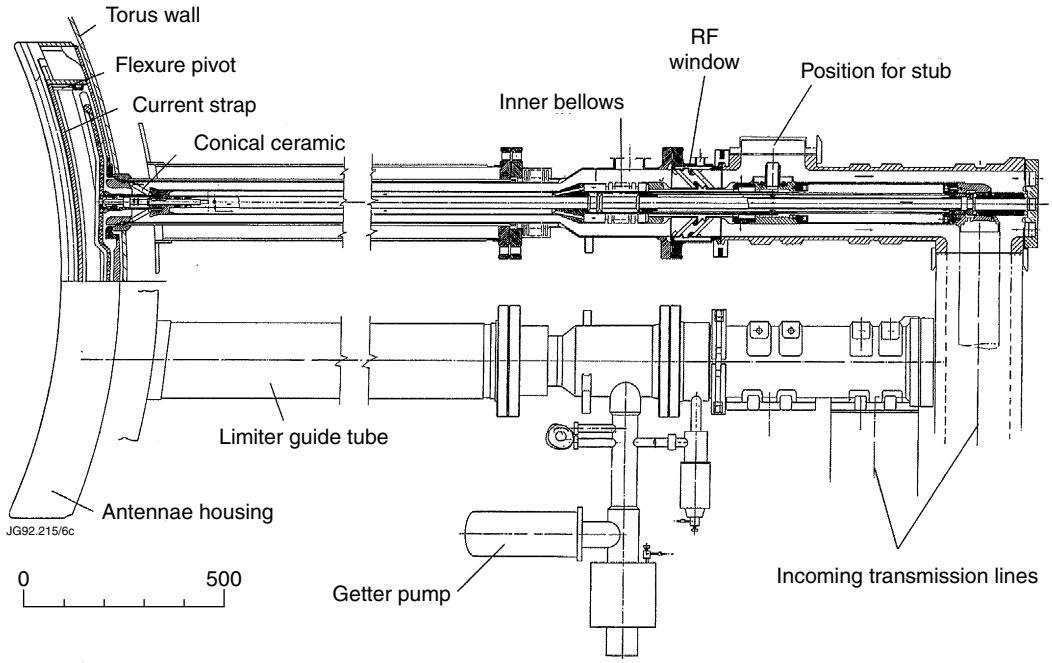

Fig 7.1: Schematic of the A1 antennae.

The present A2 antennae designed to match the MkII GB divertor configuration (Fig.7.1) do not allow the plasma volume to be increased significantly. It is therefore necessary either to re-instate the A1 antennae (Fig.7.2) used until 1991, or to make new antennae. The first option is the more conservative and ensures the use of a well-tested and successful shield for the antenna. However, the toroidal field has to be reversed. The second option may be considered in a second step.

Because of the inclination of the beryllium bars making the shield, the use of ICRH with the A1 antennae requires the toroidal field to be reversed while keeping the current in the same direction to stay in co-current for the NBI. In addition, this option would require the following modifications:

- Rotate the antenna poloidally to fit with the new external plasma shape (the curvature is not symmetrical about the centreline).
- Redesign both ends of the Vacuum Transmission Line, back to the A1 design (unless the line is being rebuilt).

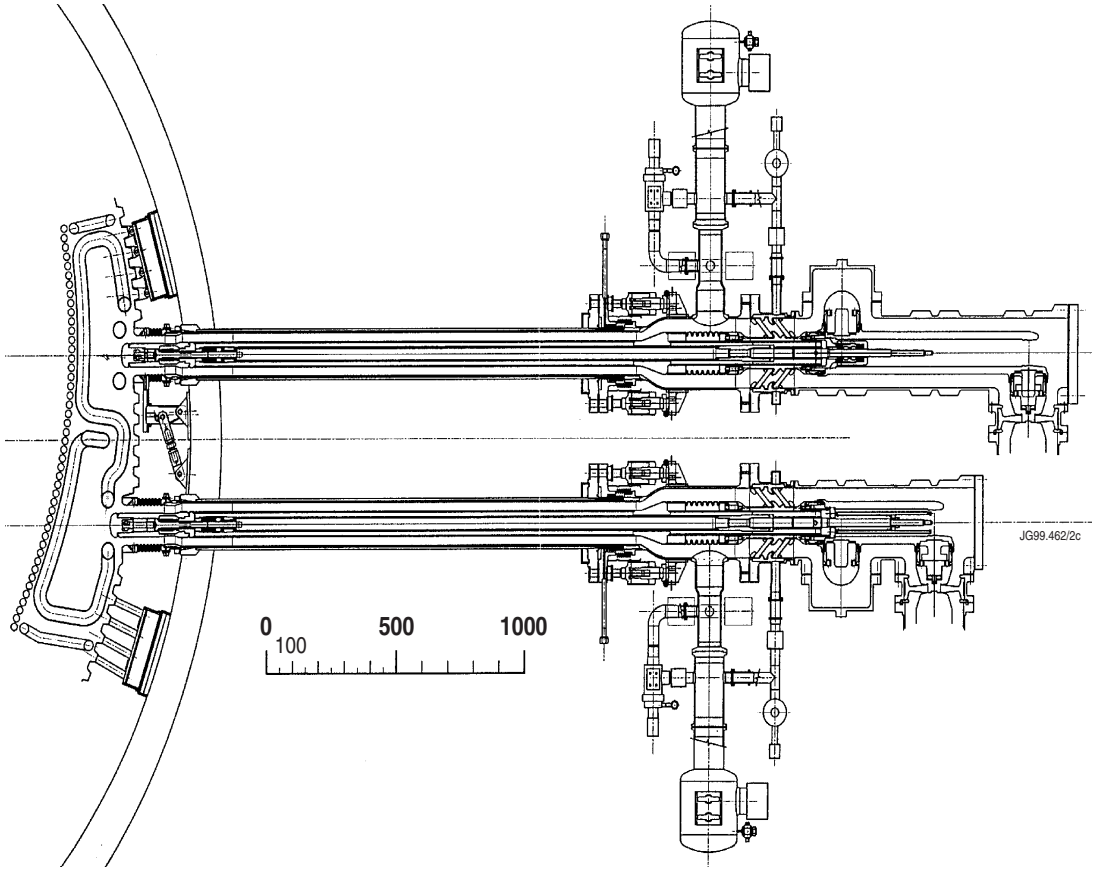

Fig 7.2: Schematic of the A2 antennae.

- Change the conical ceramic.
- Remove A2 support blocks and replace by A1 blocks.
- New protection plates are required for the top and bottom of the antennae in place of the toroidal belt limits which filled this role previously.

Other points to consider:

- It is feasible to move the A1 antenna radially, but the expected stroke will be small (a few centimetres).
- the A1 is partially compatible with remote handling.
- the NBI line-of-sight views the antenna: this may damage the antenna and was indeed observed in the past. This must be examined carefully in the design or re-use of the set of tiles protecting the antenna. The first assessment indicates that the NB of Octant 4 intercepts the picture frame of the antenna and the power load seems to be acceptable for those tiles.

For this option a 1.5 year lead time would be required for modification and testing.

The second option would require the design and construction of a new antenna. Several options can be considered according to the desired number of straps (from 1 to 4). This new antenna should have the following features:

- compatibility with a range of plasma configuration
- increase the width of the antenna to improve the coupling resistance.

- Bandwidth 25-55MHz.
- Picture frame.

7.1.2 Implications of Changing the Field Direction

In the present configuration JET has a negative Ip and a negative field. The helicity is therefore right handed. The choice to use the A1 antennae in JET, require the reversal of the toroidal field when ICRH is used because of the left-handed helicity of the shields. Reversing the field would mean to reverse the grad(B) drift direction (directing it away from the target) while keeping the current in the same direction to remain in co-injection with the neutral beam. The implications of reversing the field are as follow:

H-mode Threshold

With grad(B) away from the target, one implication is the power threshold. It can be estimated that the H mode threshold is likely to be increased by a factor 1.5 to 2. This estimate relies on the data collected with both the MarkIIA and the MarkIIGB. However, this may also help to keep the ELMy H-mode with type III ELMs at high power when operating at high triangularity. The expected energy content in Enhanced JET ELMy H-modes is increased by a factor of 3 to 4 with respect to the ELMy H-modes in the present JET. Therefore, the danger in operating at very high triangularity in ELMy H-mode is to encounter type I ELMs which would expel a significant amount of energy onto the divertor tiles and increase the power load. In addition, the vertical stabilisation system may not be able to cope with such large ELM amplitude. The vertical stabilisation system probably needs to be upgraded. Reversing the field will allow operation at higher energy content with reasonable ELM activity. It might also be useful for the optimised shear scenarios to increase the H-mode threshold in order to have lower ELM activity.

Forces

The reversal of the field does not change the direction arising from eddy currents or halo currents. However, the forces will be reversed in the divertor coils feeds. Rather than the feeds being pushed together the forces will pull them apart. Past calculations showed that these forces should be within the strength of the epoxy, binding glass tape and coil cases. Therefore, the forces do not seem to be a limitation for the operation with reversed field.

Poloidal Limiter

Reversing the field also means modifying the poloidal limiters. The tiles of this limiter are indeed designed for right handed configurations. Since those limiters are likely to be removed for JET-upgrade, this should have no consequence.

Power Deposition

In the case of the grad(B) drift towards the divertor target a 1/3 ratio is expected between the inner and outer strike zone. When the ion grad B drift direction is away from the target,

measurements are suggesting that the power loading is equalised between the inner and the outer strike zone. This should be taken into account in the design of the divertor. In addition, both strike zones will be in the same divertor regime which should ease the physics interpretation and may increase the performance of the divertor.

Error Fields

Previous calculations suggest that the n = 1 m = 2 component of the error field could be higher for left handed configurations. Therefore, it will be necessary to include error field compensation in the design of the JET Enhanced configuration.

7.2. Remote Handling and In-Vessel Work

Minimising human exposure to radiation is the primary motivation for the extensive use of remote handling inside the torus. JET has done this very successfully during the installation of in-board pellet rack in 1999. The ^{60}Co radiation arising from DTE1 together with ^{58}Co from preceding D-D operation would limit manned access to a few tens of hours per person per year. Thus the use remote handling is an essential part of any enhancement of the JET in-vessel configuration.

A preliminary assessment indicates that approximately 50% of the entries during the 16 months shutdown would be covered by remote handling. Preparatory work will be required to install a second boom (octant 1), develop new tools for the existing boom (octant 5) for handling the complex in-vessel tasks and rehearse all the in-vessel activities. According to this preliminary assessment, the shutdown can be composed of the following steps:

- The first two months of the shutdown will not require manned access. Preparations will include fitting the new boom, tiles traps, viewing cameras, lighting, making radiation surveys, samples taking and vacuum cleaning. Thereafter all divertor carriers and remotely handleable limiter protections and antennae tiles will be removed. The torus access cabin (TAC) will be fitted at octant 3 after removal of the LHCD launcher.
- The second phase, lasting 3 1/2 months, will be mainly made by remote handling removal of components (Fig.7.3). Manual work is also necessary because many of the removal tasks are either virtually impossible or require

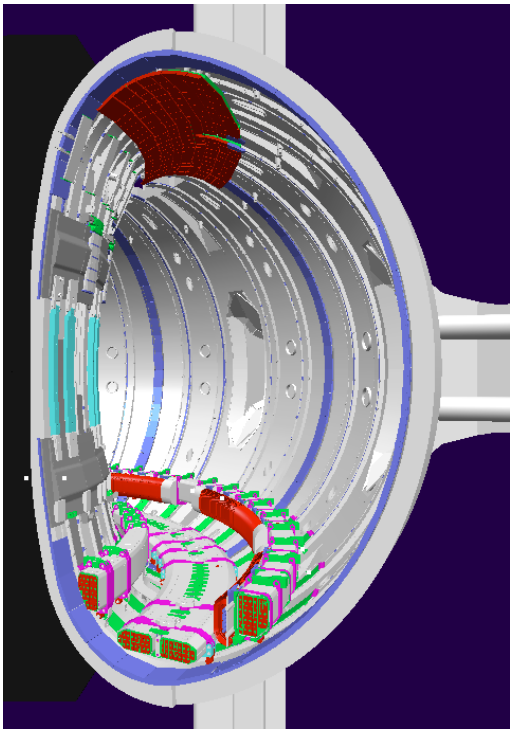

Fig 7.3: Impression of the torus after removal of first wall and divertor components.

unjustifiable use of resources if done with remote handling. This phase includes the removal of LHCD items, earth straps, protection tile supports, poloidal and guard limiters, water-pipes and french horns, ICRH antennae, saddle coils, diagnostics, aramid seals and divertor support structure.

- The installation phase will also combine manual and remote handling activities over about 7 months. Activities include the welding of support pads for wall claddings, diagnostic conduits, protection tiles, ICRH antennae and LHCD launcher. Thereafter, comes the installation of the divertor base plate, water and french horn pipes, diagnostics, divertor inner and outer rings, antennae, outer wall claddings, guard limiters, ceramid seals and earth straps. At this stage the manned access ends with the removal of the TAC from octant 3 and re-fitting the refurbished LHCD assembly.
- The final month installation phase covers the remote fitting of all tiles on wall cladding, protection brackets, saddle coils, limiters, antennae and LHCD launcher. Finally the divertor base plate and side carriers are installed (Fig.7.4).
- Removal of the booms, cameras, lightings and tools, followed by radiation surveys and other inspections completes the estimated 14 months shutdown.

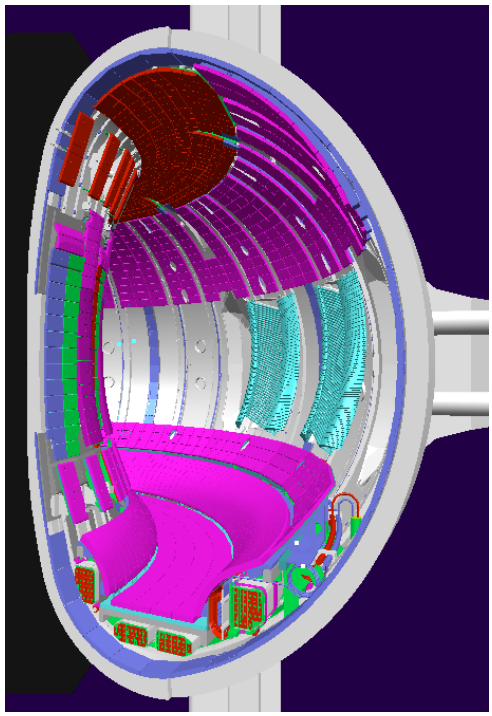

Fig 7.4: Impression of the torus after installation of in vessel Enhanced JET components.

7.3 Maximum Heat Load for the Strike Points

In JET recent measurements have suggested a relation between the temperature and the density in the scrape-off layer as:

$$n_e \propto T_e^{1/2}$$

From this relation it follows that the characteristic decay length of both the density and the temperature have the following relation: $\lambda_n = 2.\lambda_T$

From the heat transport equation in the so-called “Conductive Regime” the typical heat flux decay length λ_q can be expressed as: $\lambda_q = 2/7\ \lambda_T$

Typical λ_n in ELMy or ELM-free H-mode is 1 to 2 cm. This value is generally higher in L-mode plasmas (4 to 7 cm). Therefore, λ_q will be of the order of 5 to 10 mm. Recent measurements

are suggesting that λ_q falls when the input power is increased and can be as low as 3mm. For the present calculation 5mm will be taken for λ_q.

The flux expansion $F_{//}$ is defined as the expansion of the magnetic flux tube from the mid-plane onto the divertor. It can be approximated as:

$$F_{//} = 0.2305\ Ip/B_T/\ tg(\theta_{perp} + \alpha)$$

Where θ_{perp} is the angle of incidence of the field lines on the tile and α the inclination of the tile. Knowing the flux expansion, the wetted surface can be expressed as:

$$S = \lambda_q\ 2.\pi\ R_m\ F_{//}$$

Knowing the wetted surface at the strike points, the maximum power load at the strike points can be estimated with varying the incident angle of the field lines. From the power load q, the irradiation time required to increase the tile surface temperature by ΔT is:

$$t_{irr} = \pi/4\ (\Delta T_{surf}/\ q)^2\ \rho\ Cp\ K$$

where K is the thermal conductivity, Cp the heat capacity, and ρ the volume density of the CFC tile. Table 7.1 summarises the results for varying field line incidence:

θ_{perp} [deg]	$\lambda_q\ F_{//}$ [mm]	Power flux [MW/m^2]	Duration time for ΔT_{surf}=1200° C increase on the tile surface
0.5	200	4.9	15.4 to 27.6s
1	100	9.8	3.8 to 6.9s
2	50	19.6	0.96 to 2.7s
4	25	39.2	0.24 to 0.42s
6	16	59.4	0.1 to 0.17s

Table 7.1: Calculation made at R=2.5m for λ_q=5mm, 15MW per leg, for a 6MA / 4T plasma, α=0° and constant material properties. Initial baking temperature: 300°C.

From this table, it is clear that the angle of incident should be less than 1° to avoid excessive heat of the tile during 5 to 10s. A 5s second pulse is barely possible with θ>1°. In addition, if the incident angle is 6°, the power load can be as high as 60MW/m^2.

However two features can reduce this high power load. Firstly, under these extreme conditions, 10-15cm sweeping of the X-point should be sufficient to drop the power load down to 10MW/m^2. As already mentioned, the plasma configuration described in paragraph 3.2. is indeed compatible with sweeping the X-point. Secondly, the tile geometry and thermal properties can be optimised to reduce the local power heat flux (*see Section 5.2*). The detailed study shall consider these various parameters to minimise the heat load on divertor for a large variety of magnetic configurations.

7.4. Forces and Stresses on TF and Copper

Out-of-plane forces have been computed for the reference equilibrium presented in the previous paragraph. This calculation does not take into account the compliance of the structure. Even for this pessimistic case, the forces exerted on the collar and rings (Fig.7.5) appear to be within the allowable limits. After a disruption the transverse flux at the TF flux loop can be higher when the plasma is present. Looking at Table 7.2, the forces on the rings are indeed higher but they are still below the limits.

The TF tensile stress section of the TF coil copper can also be inferred from the same calculation. The maximum copper axial stresses are found to be within the 10,000 cycles allowable stress both on the reduced cross section of the inner leg end at the brazed joints (Table 7.3). The shear stresses in the TF insulation are also within the limits.

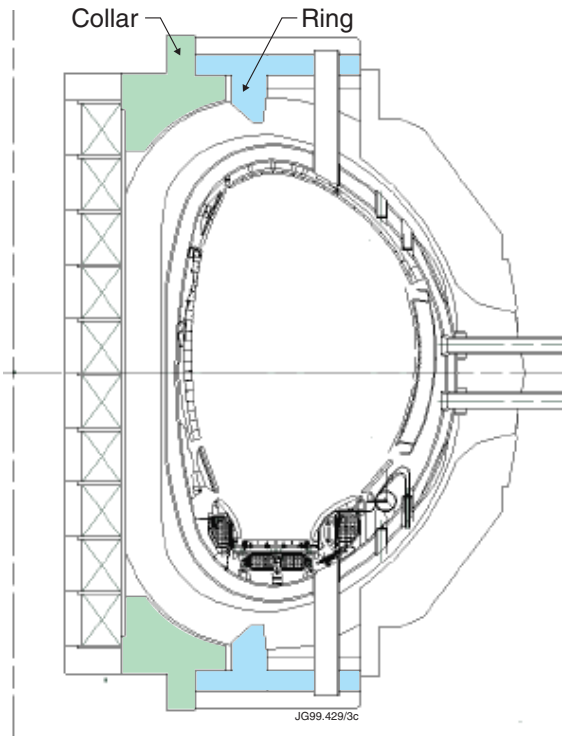

Fig 7.5: Schematic of the Enhanced JET configuration showing location of collars and rings.

	Collar Top [kN]	**[kN]**	**Ring Bottom [kN]**	**Collar Bottom [kN]**
Equilibrium	604 (650)	353 (560)	540 (560)	460 (650)
Disruption	48 (650)	503 (675)	614 (675)	466 (650)

Table 7.2: Forces on Rings and Currents for the 6MA/4T configuration (Allowable limits in brackets)

	Equilibrium	**Disruption**	**Allowable**
Inner leg [Mpa]	157	146	170
Outer leg [Mpa]	98	100	170
Brazed joints [Mpa]	81	80	130

Table 7.3: TF Copper axial stresses

From this study of the TF stresses, it can be concluded that the strongly shaped 6MA/4T configuration can be achieved in JET with acceptable forces and stresses on the TF copper and insulation on the collars and rings support structures. More calculations are in progress to perform

the calculation including compliance. The life consumption and fatigue is due to be continuously monitored against the allowable limits at peak stress.

7.5 Alpha Particle Diagnostic in an Enhanced JET

An important aspect of the exploitation of an Enhanced JET will be the diagnosis of alpha particles. Whilst great strides were made in this area during DTE1 and the DT experiments in TFTR, it is clear that this area of work is in its infancy and that much preparatory work needs to be done before a future JET DT experiment. The lead time for the preparation of major new diagnostic systems is such that an immediate start is needed in order that an effective suite of alpha diagnostics is fully commissioned ready for the DT phase of the Enhanced JET.

In order to characterise the interaction between alpha particles and plasma instabilities, it will be necessary to measure profiles of the alpha density. Preferably, it should be possible to probe the distribution function in velocity space such as the passing/trapped boundary. Both TFTR and JET used high energy NPAs to obtain some information about the distribution function of near perpendicular alphas. Spatial information was obtained in TFTR by the use of a lithium pellet as a double charge exchange source. Although this restricted the plasma conditions where measurements could be made, the effects of sawteeth on the alpha profiles were recorded. JET observed a substantial mixing between alphas, double charge exchanged off helium like impurities, and knock-on deuterons which, having the same mass and charge ratio as alphas, were detected as well. It seems likely that a strong knock-on triton signal, unpolluted by other sources, would have been observed and this offers a good way to utilise an array of NPAs.

Unless convenient and very high power microwave sources are found, the only viable collective scattering scheme for alphas is the CO_2 source. The extreme forward scattering angle means that spatial resolution will be limited. Nonetheless, serious consideration should be given to CO_2 collective scattering because it provides an absolute measurement, against which other methods can be validated.

TFTR made use of an alpha charge exchange spectroscopy system which probed the distribution function up to ~600keV. The density of epithermal ash is very sensitive to events occurring during slowing down, so that the effects of MHD activity were clearly observed. Such a method was not considered for JET because a large viewing aperture close to colinear with the neutral beam source is needed. However, given the importance of alpha physics in an Enhanced JET, this position should be reconsidered.

Lost alpha measurements are needed to test the models for first orbit loss and stochastic diffusion. Also, a direct evaluation of the localisation and power density of alphas striking the first wall should be provided. This is of particular importance in advanced regimes, where reduced core current density will almost certainly enhance alpha losses. Both JET and TFTR used in-vessel detectors which subtended a tiny proportion of the first wall area. TFTR deployed theirs much more successfully and much useful physics was done. Following JT60U's success in

measuring lost NBI ions using an IR camera system, a design study was carried out for detecting alphas in this way in TFTR. Whilst too late to be implemented, the study showed that this would be a viable technique and, given the large first wall area covered by this, it is proposed that such a system should be installed on JET. It would also provide a good monitor of plasma-wall interaction, since the IR region is much less polluted with impurity lines than the visible region.

Finally, active TAE spectroscopy should be reconsidered. Whilst systems will be in place for passive TAE spectroscopy, the stabilising effect of slowing down neutral beam ions implies that instability will only be seen in rather unusual circumstances. Excitation of the modes by an external source would allow their damping rate to be determined and tested against theoretical modes. Thus, an antenna for n~5 TAEs is needed and urgent consideration should be given to preparing one.

CONCLUSIONS

This report has demonstrated the wide potentials that the JET facility could offer to address crucial questions like scenario validation, confinement study and burning plasma physics issues in support for next step devices. To achieve this task, JET would require the modification of the in-vessel configuration without changing the divertor coils combined with additional heating upgrades.

The procurement of an extra 20MW of additional heating power is required for exploiting fully the confinement capability of the JET device. This could be achieved by a combination of methods to be chosen among NBI, ICRH, ECRH and N-NBI. In the next two or three years both Neutral Beams Injection and the ICRH antennae could provide an increase of the power of 8 to 10MW in total. In addition, recent developments of ECRH and negative Ion sources are making these heating systems serious candidates to provide additional plasma heating and non-inductive current control capabilities.

The refurbishment of the in-vessel components and the design of a new divertor can provide a volume increase of about 30%. With this arrangement, 6MA/4T configurations could be devised with a triangularity of 0.6 and a volume approaching 110m3. For these configurations forces and stresses in the toroidal coils are staying within the allowable limits. Transport simulations and scaling extrapolation are both indicating that the confinement could be doubled and fusion energy yield in the range of 100MJ during a single pulse in a quasi steady state discharge would become possible. Fusion gain as high as 2 could also be achieved transiently and for those the core electron heating would be essentially provided by the alpha particles.

With plasmas close to burning conditions, reactor physics issues could already be addressed in the enhanced JET in preparation for the operation of an ITER class device. Alpha heating and collective alpha-driven instabilities are particularly relevant. Macroscopic ideal and non-ideal MHD phenomena at high internal pressure, tritium retention and fuelling, transport physics and scalings, feedback control and power heat loads would be the other main areas for investigation.

For all these topics the JET enhanced could extend the knowledge or provide relevant answers in the context of burning plasmas.

To make these studies possible, the divertor is to be modified on the basis of the past JET experience on divertor design. The new divertor is due to preserve the X-point control and the pumping capabilities, but would allow a large variety of plasma configurations. It would be designed to handle 30MW of convected and conducted power for more than 5s. Some components would be removed to give room to the plasma on the outboard side. In particular, the present poloidal limiters, the saddle coils would be removed and the ICRH antennae would be replaced. These in-vessel tasks are planned to make extensive use of the remote handling during a shutdown which should extend over a period somewhat longer than one year.

Such enhancements to the JET facility would significantly improve the present knowledge of burning plasmas and would pave the way for future large experiments. The time schedule associated with the proposed modifications (about 3 years from the decision) is well matched with the time scale necessary for the construction of a next step device.

REFERENCES

[1] ITER Physics Report, to be published in Nuc. Fus. (Special Issues).

[2] Keilhacker M et al, Nucl Fusion, **39**, 189 (1999).

[3] Jacquinot J et al, Nucl Fusion, **39**, 209 (1999).

[4] Thomas P et al, Phys Rev Lett, **80**, 5548 (1998).

[5] Horton LD et al, submitted to Nuclear Fusion.

[6] Gormezano C Phys Rev Lett, **80**, 5544 (1998).